Consistent estimation of complete neuronal connectivity in large neuronal populations using sparse "shotgun" neuronal activity sampling

Yuriy Mishchenko

Journal of Computational Neuroscience

ISSN 0929-5313
Volume 41
Number 2

J Comput Neurosci (2016) 41:157-184
DOI 10.1007/s10827-016-0611-y

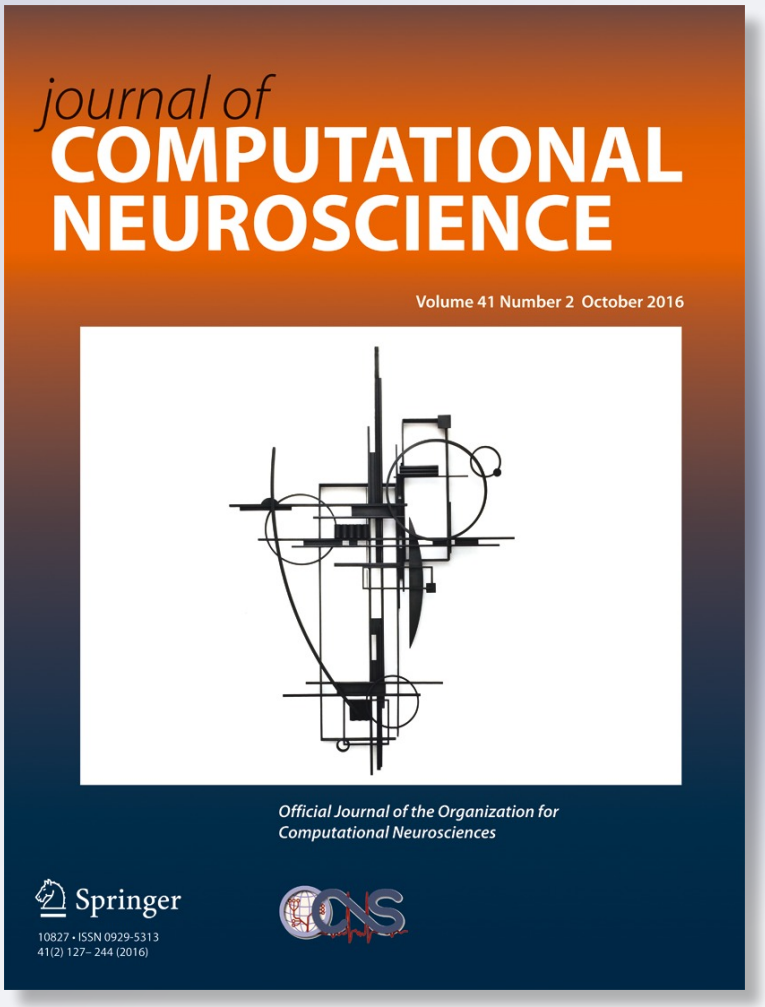

Springer

J Comput Neurosci (2016) 41:157–184
DOI 10.1007/s10827-016-0611-y

Consistent estimation of complete neuronal connectivity in large neuronal populations using sparse "shotgun" neuronal activity sampling

Yuriy Mishchenko[1]

Received: 3 February 2015 / Revised: 9 June 2016 / Accepted: 13 June 2016 / Published online: 11 August 2016

Abstract We investigate the properties of recently proposed "shotgun" sampling approach for the common inputs problem in the functional estimation of neuronal connectivity. We study the asymptotic correctness, the speed of convergence, and the data size requirements of such an approach. We show that the shotgun approach can be expected to allow the inference of complete connectivity matrix in large neuronal populations under some rather general conditions. However, we find that the posterior error of the shotgun connectivity estimator grows quickly with the size of unobserved neuronal populations, the square of average connectivity strength, and the square of observation sparseness. This implies that the shotgun connectivity estimation will require significantly larger amounts of neuronal activity data whenever the number of neurons in observed neuronal populations remains small. We present a numerical approach for solving the shotgun estimation problem in general settings and use it to demonstrate the shotgun connectivity inference in the examples of simulated synfire and weakly coupled cortical neuronal networks.

Keywords Functional connectivity · Neuronal circuit reconstruction · Calcium imaging · Neuronal population activity

Action Editor: Rob Kass.

✉ Yuriy Mishchenko
yuriy.mishchenko@gmail.com

[1] Izmir University of Economics, Izmir, Turkey

1 Introduction

Recent advances in multi-neuronal activity recordings using calcium-sensitive fluorescence imaging have made it possible to image the activity of large neuronal populations over extended periods of time (Tsien 1989; Yuste et al. 2006; Cossart et al. 2003; Ohki et al. 2005; Reddy et al. 2008a; Grewe et al. 2010). Bulk-loading of organic calcium-sensitive fluorescent dyes offers the fluorescent signal-to-noise ratio (SNR) sufficient for resolving individual action potentials (spikes) of neurons (Yuste et al. 2006; Stosiek et al. 2003) and genetically encoded calcium indicators are approaching the SNR levels necessary for neuronal activity imaging with single spike accuracy (Wallace et al. 2008). Modern cooled CCD-microscopy can allow imaging of calcium fluorescence in neuronal populations *in-vitro* with frame-rates of over 60 Hz (Djurisic et al. 2004) and 2-photon laser scanning microscopy offers similar frame-rates *in-vivo* (Iyer et al. 2006; Salome et al. 2006; Reddy et al. 2008b; Cotton et al. 2013; Theis et al. 2015). These advances now allow studying the single-cell structure of neuronal circuits in the brain using accurate statistical approaches (Pillow et al. 2008; Stevenson et al. 2008a, b; Stevenson et al. 2009; Mishchenko et al. 2011).

One of the biggest challenges faced by the functional analysis of neuronal connectivity in the brain remains the presence of unobserved or hidden inputs in the observed neuronal population activity (Nykamp 2007; Pillow and Latham 2007; Vidne et al. 2009). Because functional connectivity analysis relies on correlating the activity of different neurons in a neuronal population over extended periods of time, the presence of unobserved inputs can contribute errors to such inference. In particular, the classical "common inputs" scenario causes one to mistake the correlations observed between two neurons because of their

correlated hidden inputs for a direct connection between them (Nykamp 2005, 2007; Kulkarni and Paninski 2007; Pillow and Latham 2007). Despite rapid progress in experimental neuronal population activity imaging methods, the simultaneous observation of the activity of all neurons with required temporal resolution even in the smallest of neuronal circuits is currently not feasible, and the development of robust computational techniques for overcoming the hidden inputs problem remains one of important open questions in computational neuroscience (Nykamp 2005, 2007; Kulkarni and Paninski 2007; Pillow and Latham 2007; Vidne et al. 2009; Keshri et al. 2013).

Recently a promising approach for overcoming the hidden inputs problem—the shotgun sampling—had been proposed in (Turaga et al. 2013; Keshri et al. 2013; Soudry et al. 2015). In this approach, neurons in a large neuronal population are proposed to be imaged randomly in small groups, whereas the connectivity matrix of the complete neuronal population is assembled statistically by combining the information about the neuronal connectivity contained in different such partial measurements. The shotgun approach offers the possibility of reconstructing the connectivity in large neuronal circuits by using limited imaging resources, without the need to simultaneously image the entire neuronal circuit.

In this paper, we perform a systematic analysis of certain aspects of the shotgun sampling proposal such as the asymptotic correctness of the respective connectivity estimator, the expected speed of convergence, and the necessary data sizes. (Keshri et al. 2013; Soudry et al. 2015) perform a numerical demonstration of the shotgun connectivity estimation approach using simulated models. However, it may not be clear right away if the shotgun connectivity estimation must really be free from the hidden inputs problem. One may observe that, even as all neurons in a neuronal population do get imaged with this approach over different points of time, the observations still fail to provide a complete picture of the input-output relationships for even a single neuron in the population: the total number of neurons that need to be simultaneously imaged to observe all the inputs of even a single neuron in mammalian cortex can be as high as 10,000. Without having the information about the complete set of inputs and outputs of any single neuron in a circuit, one may wonder if the hidden inputs problem will really be resolved. Furthermore, if the shotgun approach does allow the unambiguous determination of the connectivity matrix in a complete neuronal circuit, what are the trade-offs that had been made? In particular, what is the minimal imaging time required for a given accuracy of the connectivity matrix estimation and how does this time scale with the size of the unobserved neuronal populations, observations' sparseness, and other parameters?

In this work, we show that the shotgun approach can be indeed expected to allow recovering the complete connectivity matrix in statistical neuronal activity models under some rather general conditions. We estimate the speed of convergence of the shotgun connectivity estimation and show that the imaging time required to achieve a given accuracy in the shotgun estimation scales proportionally to the number of neurons in the unobserved neuronal populations as well as the square of the typical connectivity strength and the inverse square of the fraction of neurons contained in a typical observation. This scaling is inopportune for the reconstructions of neuronal connectivity in the experiments where the number of unobserved neurons will remain large or the fraction of observed neurons will be small. We also present a numerical approach for solving the connectivity estimation problem in general neuronal population activity models using the shotgun imaging experiments, and demonstrate its applications to the shotgun connectivity estimation in simulated small realistic neuronal networks.

We focus in this paper specifically on the problem of inference of underlying neuronal connectivity matrix from sparse neuronal activity observations. In the case of fluorescent calcium imaging—currently the most plausible modality for collecting large scale neuronal population activity data—another important component of such inference is the deconvolution of calcium fluorescence signal into underlying neuronal spike trains. In recent years, significant progress had been achieved with respect to this deconvolution problem, for example, see (Theis et al. 2015) for a benchmark and a survey of such modern deconvolution approaches. At the same time, experimental trials indicate that existing calcium signal deconvolution methods may still need significant improvements to allow robust use in practice (Cotton et al. 2013; Theis et al. 2015). Nonetheless, in this paper we do not consider this important aspect of the analysis of calcium imaging data. Instead, we focus on the mathematical and computational problems of specifically the neuronal connectivity estimation from the shotgun imaging data, assuming that the deconvolved neuronal activity had been made available by other means or that an effective neuronal connectivity model is used to describe the continuous calcium fluorescence signal. In the future, the incorporation and the impact of the calcium signal deconvolution problem to functional inference of neuronal connectivity will require more detailed investigation, including the impact on the inference of increased uncertainties in spike timings (such as extracted from low frame-rate calcium imaging data), apparent possibility of high fractions of lost spikes in existing calcium signal deconvolution methods (Cotton et al. 2013) and their vulnerability to overestimating bursting and underestimating isolated neuronal spiking (Theis et al. 2015).

It should be emphasized that while (Keshri et al. 2013; Soudry et al. 2015) consider the shotgun connectivity estimation numerically in one statistical model and demonstrate its empirical utility by means of simulations, this paper presents theoretical results about the shotgun connectivity estimation that apply to a broad family of models. That notwithstanding, the model considered in (Keshri et al. 2013; Soudry et al. 2015) is not specifically in the family considered here, as it includes terms for time-varying external stimulus inputs, which are not treated in this work.

The remainder of the paper is organized as follows. In Materials and Methods, Section 2.1, we review the shotgun neuronal connectivity estimation problem and introduce some notation and mathematical formalism. In Section 2.2, we discuss the class of statistical models of spontaneous neuronal population activity considered in this work. In Section 2.3, we present a numerical EM algorithm for solving the shotgun connectivity estimation problem in general causal models of neuronal population activity. In Section 2.4, we present the details of our numerical simulations.

In Results, Section 3.1, we present theoretical arguments that "shotgun-like" neuronal activity imaging experiments can be expected to allow the recovery of complete connectivity in large neuronal populations very generally, as long as certain conditions are satisfied by the set of neuronal subpopulations covered during sparse neuronal activity imaging. We also present a more detailed analysis of the shotgun connectivity estimation in linear, exponential generalized linear, and generalized linear models of neuronal activity. In Section 3.2, we build on the results of Section 3.1 to demonstrate that the shotgun neuronal activity imaging can be organized in a different and far more advantageous way, both from the point of view of experimental implementations and the data analysis. In Sections 3.3 and 3.4, we describe the shotgun connectivity estimation in simulated linear and more realistic generalized linear neuronal network models. Discussion and conclusions follow in Section 4.

2 Materials and methods

2.1 The shotgun sampling approach for neuronal connectivity inference

In the shotgun sampling, one's objective is to recover the effective connectivity matrix of a large neuronal population using a collection of partial samples of the activity of that population's different subpopulations. One simple way to visualize this idea is to think about reconstructing a large image by using small fragments of that image obtained from its different locations.

More formally, we define the effective connectivity matrix $\mathcal{W}$ as a parameter of a statistical model of neuronal population activity, $P(\mathcal{X}|\mathcal{W})$, where $\mathcal{X}$ stands for the raster of the historical activities of the neurons in a neuronal population and $P(\mathcal{X}|\mathcal{W})$ stands for the likelihood of observing a particular raster of neuronal activity $\mathcal{X}$ given $\mathcal{W}$. In network models of neuronal activity, $\mathcal{W}$ typically is a matrix $\mathcal{W} = (w_{ij})$ having as many rows and columns as there are neurons in the population, N, and where each element w_{ij} characterizes the impact of the past activity of one "input" neuron j on the activity of one "output" neuron i. Our objective, therefore, is to estimate the complete connectivity matrix $\mathcal{W}$ given only partial views of the neuronal activity raster $\mathcal{X}$.

In the context of this problem, we introduce below the following notations. We denote the raster of the activities of the entire neuronal population (that is, both observed and unobserved or hidden) over all observations by the subscript-less symbol $\mathcal{X}$. We denote the activity of the entire neuronal population during a single observation t by the symbol $\mathcal{X}_t$. Thus, $\mathcal{X} = \{\mathcal{X}_t, t = 1 \dots T\}$, where T is the total number of observations.

Similarly, we denote the collection of all neuronal activities that had been observed by the subscript-less symbol X. The activity of all observed neurons during a single observation t is denoted by the symbol X_t, respectively, so that $X = \{X_t, t = 1 \dots T\}$. Finally, the collections of unobserved neuronal activities over all and a single observation are denoted by the symbols Y and Y_t, respectively, and likewise $Y = \{Y_t, t = 1 \dots T\}$.

We now formally state the shotgun estimation problem as the problem of estimating the effective connectivity matrix $\mathcal{W}$ of a statistical model of neuronal population activity $P(\mathcal{X}|\mathcal{W})$ given a set of partial observations of that model's activity X.

For greater simplicity of the discussion to follow, in a significant part of this manuscript we will focus on the shotgun connectivity estimation formulated for a single output neuron and a population of neuronal inputs that is observed sparsely. In this picture, the output neuron is continuously monitored while the set of the observed input neurons changes. This assumption allows for a significant simplification of the arguments while not causing any significant loss of generality. The latter is because in a typical network model of neuronal activity the activities of individual neurons are conditionally independent given the activity of the presynaptic neuronal populations and the respective input connection weights. In other words, the full likelihood $P(\mathcal{X}|\mathcal{W})$ in such models factorizes over the rows of the connectivity matrix $\mathcal{W}$,

$$P(\mathcal{X}|\mathcal{W}) = \prod_{i,t} P(\mathcal{X}_{it}|\{\mathcal{X}_{t'}, t' < t\}; W_i), \tag{1}$$

where $W_i = \{w_{ij}, j = 1 \ldots N\}$. Thus, it is always possible to consider the estimation of $\mathcal{W}$ as such done one row W_i at a time.

To summarize the notation conventions to be consistently followed in this paper, the script symbol $\mathcal{W}$ will always refer to the complete connectivity matrix of an entire neuronal population, while the symbol W_i will always refer to a single row of that matrix defined by all input connection weights of one neuron. The symbol w_{ij} will refer to a single connection weight from $\mathcal{W}$ corresponding to one output neuron i and one input neuron j.

The script symbols $\mathcal{X}$ and $\mathcal{X}_t$ will be used to refer to the neuronal activity of the entire neuronal population, whereas the plain symbols X, X_t, Y, and Y_t will be always used to refer to the observed and the unobserved parts of that population's activity, respectively. We will sometimes make use of the symbols X_t and Y_t to refer to the set of neurons contained in X_t or Y_t, as opposed to their actual activities. This distinction will be always made clear in the context. Finally, we will always understand $\mathcal{X}_t$, X_t and Y_t to be column-vectors, and W_i will always be a row-vector.

2.2 Statistical causal models of neuronal population activity

In Section 2.1, the model of neuronal population activity was specified as a general parametric model describing the probability of the realizations of different neuronal activity rasters $\mathcal{X}$, $P(\mathcal{X}|\mathcal{W})$. However, in neuroscience one is frequently interested in the models of neuronal activity that are causal in nature. Such models can be formulated in terms of general Markov models such as described by the relationship

$$\mathcal{X}_t \sim P(\mathcal{X}_t|\mathcal{X}_{t-1}; \mathcal{W}), \tag{2}$$

where $\mathcal{X}_t$ is the activity of the neuronal population at time t and $P(\mathcal{X}_t|\mathcal{X}_{t-1}; \mathcal{W})$ is the probability of the realization of the activity pattern $\mathcal{X}_t$ given one previous state of the neuronal population $\mathcal{X}_{t-1}$ and the model parameter $\mathcal{W}$. It may need to be pointed out that $\mathcal{X}_t$ may need to refer to a more general neuronal state than such described by only the spike raster or the firing rates of neurons. Namely, $\mathcal{X}_t$ may be required to also contain the quantities such as the membrane potentials, synaptic currents, and other internal parameters of neurons whose evolution determines the spiking rates. In terms of such a "generalized" state, however, any causal model of neuronal activity can be represented as the model defined by Eq. (2).

In this work, we focus on two specific cases of the general model (2): the linear model of neuronal activity and the generalized linear model (GLM) of neuronal activity, to be discussed in greater detail below.

2.2.1 The linear model of neuronal activity

The linear model of neuronal activity is a simple model where input and output neuronal activities are related linearly. Neurophysiologically such a model can describe the evolution of suitably smoothed firing rates in a neuronal population or the evolution of directly the $\Delta F/F$ calcium signal variables associated with that firing rates, in an effective model sense. For the purpose of this paper, the linear model of neuronal activity presents the key advantage of allowing the analysis of the shotgun connectivity estimation to be carried out analytically.

More specifically, in the linear neuronal activity model the activity of a neuronal population is modeled by using a set of continuous activity measures $\mathcal{X}_t$, which can be interpreted as appropriately smoothed neuronal firing rates or calcium imaging signals, as described above. The input-output relationship between these variables is

$$\mathcal{X}_{t+1} = \mathcal{W}\mathcal{X}_t + \epsilon_t. \tag{3}$$

Here, $\mathcal{X}_t$ is an N-element column-vector encoding the activity of a population of N neurons and the index t plays the role of discrete time. The parameter $\mathcal{W}$ is a $N \times N$ connectivity matrix, and ϵ is an i.i.d. normal random noise variable. Without loss of generality, we can assume ϵ to have the variance of one, so that the model probability densities $P(\mathcal{X}_t|\mathcal{X}_{t-1}; \mathcal{W})$ and $P(\mathcal{X}|\mathcal{W})$ are given by

$$P(\mathcal{X}_t|\mathcal{X}_{t-1}; \mathcal{W}) \propto \exp(-(\mathcal{X}_t - \mathcal{W}\mathcal{X}_{t-1})^2/2) \tag{4}$$

and

$$P(\mathcal{X}|\mathcal{W}) \propto P(\mathcal{X}_{t=1}) \exp\left(-\sum_{t=2}^{t=T} (\mathcal{X}_t - \mathcal{W}\mathcal{X}_{t-1})^2/2\right), \tag{5}$$

where $P(\mathcal{X}_{t=1})$ is a prior for the first bin of the neuronal activities.

2.2.2 The generalized linear model of neuronal activity

The generalized linear model (GLM) of neuronal activity is a general powerful class of statistical models of spiking neuronal population activity described as a system of coupled inhomogeneous Poisson processes. GLM has been used in the literature quite extensively to model the statistical properties of individual neurons as well as large neuronal populations (Brillinger 1988; Chornoboy et al. 1988; Brillinger 1992; Plesser and Gerstner 2000; Paninski et al. 2004; Paninski 2004; Rigat et al. 2006; Truccolo et al. 2005; Nykamp 2007; Kulkarni and Paninski 2007; Pillow et al. 2008; Vidne et al. 2009; Stevenson et al. 2009).

In this work, we consider two forms of such GLM of neuronal activity. The first GLM is defined by the inhomogeneous Poisson process described by

$$P\{\mathcal{X}_{it} = s\} = (\lambda_{it})^s e^{-\lambda_{it}}/s!,$$
$$\lambda_{it} = f\left(b_i + \sum_{j=1}^{N} w_{ij}\mathcal{X}_{j,t-1}\right)\Delta t, \tag{6}$$

where the neuronal activity variables $\mathcal{X}_{it}$ are the Poisson random variables indicating the spike count of different neurons $i = 1, 2, \ldots, N$ in different time bins t of size Δt, b_i are constant offset parameters, and w_{ij} are coupling weights parameters. $f(.)$ is a nonlinear rate function. The diagonal weights w_{ii} can be used to model self-interactions that can exist in neuronal spike trains, such as refractory periods, burst firing, periodic firing, etc., and the off-diagonal weights w_{ij} model the interactions between the neurons. Longer time-dependencies can be incorporated in model (6) by concatenating into the state-vector $\mathcal{X}_t$ the neuronal spikes from more distant previous times. The GLM of this form is used in Section 3.1 to obtain certain theoretical results.

The second GLM form is defined by

$$P\{\mathcal{X}_{it} = s\} = (\lambda_{it})^s e^{-\lambda_{it}}/s!,$$
$$\lambda_{it} = f\left(b_i + \sum_{j=1}^{N} w_{ij} J_{jt}\right)\Delta t, \tag{7}$$

where the driving currents

$$J_{jt} = a_j J_{j,t-1} + \mathcal{X}_{j,t-1} + \epsilon_{jt}. \tag{8}$$

are autoregressive processes with certain decay constants a_j and normal noise $\epsilon_{jt} \sim N(0, \sigma_j^2)$. This model may be more advantageous in certain practical scenarios, where J_{jt} can be used to model realistic synaptic currents of different neurons. More than one autoregressive current may be defined per neuron, thus allowing this model to describe complex neuronal responses as the combinations of J_{jt}'s with different time decays. The model given by Eq. (7) reduces to the model given by Eq. (6) when $a_j, \sigma_j = 0$. Conversely, the model given by Eq. (6) can be extended approximately to the model given by Eq. (7) by concatenating into $\mathcal{X}_t$ neuronal spikes from more distant past times. The GLM of form (7) is used in the numerical simulations in Section 3.4.

The probability densities $P(\mathcal{X}_t|\mathcal{X}_{t-1})$ and $P(\mathcal{X})$ in the models described by Eq. (6) and Eq. (7) are given by

$$P(\mathcal{X}_t|\mathcal{X}_{t-1}; b, \mathcal{W}) = \prod_{i=1}^{i=N} \frac{\lambda_{it}^{\mathcal{X}_{it}} e^{-\lambda_{it}}}{\mathcal{X}_{it}!} \tag{9}$$

and

$$P(\mathcal{X}|b, \mathcal{W}) = P(\mathcal{X}_{t=1}) \prod_{t=2}^{t=T} \prod_{i=1}^{i=N} \frac{\lambda_{it}^{\mathcal{X}_{it}} e^{-\lambda_{it}}}{\mathcal{X}_{it}!}, \tag{10}$$

where $P(\mathcal{X}_{t=1})$ is a prior for the first bin of the neuronal activities.

2.3 The numerical solution of the shotgun connectivity estimation problem using the Expectation Maximization algorithm

The problem of estimating the effective connectivity matrix $\mathcal{W}$ from the shotgun sampling data in realistic settings will require numerical solution. In this section, we present a numerical approach for solving this problem in the general case of a causal neuronal activity model such as described by Eq. (2) using the Sequential Monte Carlo method and the Expectation Maximization algorithm (Dempster et al. 1977). Our development of the numerical algorithm here is carried out primarily with spiking neuronal activity models in mind, such as described in Section 2.2.2, in which case the state space $\mathcal{X}_t$ is necessarily finite. In that case, the shotgun imaging data can be treated as a Hidden Markov Model with the unobserved neuronal populations constituting the hidden states and the activities of the observed neuronal populations constituting the observations. The algorithm developed in this section also can be applied for the models of neuronal population activity with neuronal activity measured in terms of continuous variables, such as in Section 2.2.1, understood as continuous state-space Markov models, for example, such as described in (Kantas et al. 2009).

To briefly recap, the EM algorithm produces a sequence of parameter estimates $\hat{\mathcal{W}}^k$ for a parametric model $P(\mathcal{X}|\mathcal{W})$ with missing data Y with uniformly increasing likelihoods of the observed data $P(X|\hat{\mathcal{W}}^k)$, guaranteeing at least a locally-maximum likelihood estimate of $\mathcal{W}$ given X. The sequence of $\hat{\mathcal{W}}^k$ is produced by iteratively maximizing the functions

$$Q(\mathcal{W}|\hat{\mathcal{W}}^k) = E_{P(Y|X,\hat{\mathcal{W}}^k)}[\log P(X, Y, \mathcal{W})], \tag{11}$$

where $P(Y|X; \hat{\mathcal{W}}^k)$ is the posterior distribution of the hidden data given available observations X and the available parameter estimate $\hat{\mathcal{W}}^k$. This maximization is typically realized by constructing M samples of the missing data Y^l from $P(Y|X; \hat{\mathcal{W}}^k)$ and calculating $Q(\mathcal{W}|\hat{\mathcal{W}}^k)$ as $Q(\mathcal{W}|\hat{\mathcal{W}}^k) = \frac{1}{M}\sum_l \log P(X, Y^l; \mathcal{W})$.

To apply the EM algorithm here, we reformulate the shotgun connectivity estimation problem in model (2) as a Hidden Markov Model (HMM) in which the unobserved neuronal activities Y_t are treated as the hidden states and the observed activities X_t are treated as the observations. To implement the EM algorithm, we first construct a sample of the missing neuronal activities Y given X and the current estimate of the neuronal activity model $\hat{\mathcal{W}}^k$. This sampling problem can be stated as drawing a sample of hidden state sequences Y_t from the above HMM given the observations X. This sampling problem can be solved efficiently by using the standard forward-backward algorithm (Rabiner

1989; Paninski et al. 2010) implemented using the sequential Monte Carlo method (Kantas et al. 2009). Assuming such sample $Y \sim P(Y|X; \hat{\mathcal{W}}^k)$ had been constructed, we evaluate $Q(\mathcal{W}|\hat{\mathcal{W}}^k)$ by using

$$Q(\mathcal{W}|\hat{\mathcal{W}}) = \log P(\mathcal{W}) + E[\log P(\mathcal{X}_0)] + \sum_t E[\log P(\mathcal{X}_t|\mathcal{X}_{t-1}; \mathcal{W})], \quad (12)$$

where the expectation values are with respect to the produced sample of Y. $Q(\mathcal{W}|\hat{\mathcal{W}})$ can be made convex with a suitable choice of the causation in Eq. (2)—for instance, by using log-concave rate functions f in Eq. (6) or Eq. (7). If the latter is achieved, then the maximum of $Q(\mathcal{W}|\hat{\mathcal{W}})$ can be found efficiently and for very large neuronal population sizes by using standard gradient descent algorithms (Paninski 2004).

Further details of the implementation of the EM algorithm for the shotgun connectivity estimation are presented in Appendix A.

2.4 Numerical simulations

We performed numerical simulations of the shotgun connectivity estimation in linear and generalized linear neuronal activity models. In each simulation, a sparse observation of the activity of a neuronal network was simulated using the linear or the generalized linear neuronal activity model in Section 2.2, and the estimation of the network's connectivity matrix was performed using the EM algorithm of Section 2.3. The details of these simulations are presented below.

2.4.1 Numerical simulations of the shotgun connectivity estimation in the linear neuronal activity models

In the simulations using the linear model, the activity of a model neuronal population of $N = 100$ neurons was simulated using Eq. (3) with the connectivity described by a sparse random matrix $\mathcal{W}$ with sparseness $s = 0.1$ and the nonzero values that were initially distributed uniformly on the interval $[0, 1]$. For $\mathcal{X}_t$ to not diverge to infinity, the largest right eigenvalue of the connectivity matrix $\mathcal{W}$ needs to remain below 1. To insure this, the connectivity matrix $\mathcal{W}$ was divided after the generation by a number selected in such a way that the largest eigenvalue of $\mathcal{W}\mathcal{W}^T$ was made equal to a random number chosen priorly uniformly on [0,1]. The observations X were then produced using this setup by observing the activity of one output neuron continuously and the remainder input neurons in the block-wise round-robin manner described in Section 3.2. The row-vector of the input connection weights of the observed neuron was numerically estimated from the simulated data using an implementation of the EM algorithm in Matlab, following the discussion of Section 2.3, with the size of the EM sample of hidden neuronal activities $M = 100$. The parameters of these simulations are listed in Table 1.

Table 1 The parameters of the linear neuronal activity models simulated in this paper

Number of neurons	100
Connectivity sparseness	10 %
Max observation duration	500 samples
Neurons per imaging block	20 %
Imaging strategy	block-wise round-robin

2.4.2 Numerical simulations of the shotgun connectivity estimation in the generalized linear neuronal activity models

We performed more realistic numerical simulations of the shotgun connectivity estimation using two GLM neuronal networks—a small model synfire network with large long-range correlations known to be detrimental to functional connectivity estimation and a realistic model of weakly coupled network of cortical neurons.

The synfire network was simulated with the objective to confirm the resolution of the canonical common inputs problem in the shotgun approach. The synfire model was prepared as an all-excitatory network of $N = 10$ neurons with strong feed-forward connectivity pattern (see Fig. 4). All connections were generated with a large constant strength W_{syn} chosen in such a way that the probability of a post-synaptic neuronal spike conditional on the spike of any connected pre-synaptic neuron was greater than 80 %. The activity in that model was simulated using Eqs. (7–8) with the parameters chosen as in Table 2. Observations data was assembled using the block-wise round-robin sampling strategy described in Section 3.2.

The model of a realistic weakly coupled cortical neuronal network was adopted from (Mishchenko et al. 2011) and

Table 2 The parameters of the synfire GLM model simulated in this paper

Number of neurons	10
Base firing rate ($\exp(b_i)$)	15 Hz
Actual average firing rate	33 Hz
Simulation time step	1 msec
Max observation duration	50 sec
Neurons per imaging block	20 %
Imaging strategy	block-wise round-robin
Excitatory conn. strength (w_{ij})	13
Excitatory PSP rise time	1 msec
Excitatory PSP decay time	1 msec
Refractory time	1 msec

was intended to confirm the shotgun connectivity estimation in more realistic settings. The model network faithfully reproduced the experimental data available about cortical neuronal micro-circuits in literature (Braitenberg and Schuz 1998; Gomez-Urquijo et al. 2000; Lefort et al. 2009; Sayer et al. 1990). Specifically, the neuronal population was prepared as 80 % excitatory and 20 % inhibitory. The neurons were sparsely connected with each other randomly and homogeneously, with the probability of a connection between any two neurons of 10 %. The strength of the excitatory connections was set using the peak excitatory post-synaptic potential (PSP) values randomly chosen from an exponential distribution with mean 0.5 mV (Lefort et al. 2009; Sayer et al. 1990). The strength of the inhibitory connections was set using a similar exponential distribution with the mean chosen so as to balance the average excitatory and inhibitory inputs in the network (Abeles 1991). The Dale's law was respected when assigning connection strengths, that is, an excitatory neuron only had excitatory outgoing connections and an inhibitory neuron had only inhibitory outgoing connections. All neurons were given refractory periods of 1 msec enforced via a self-current J_{it} with the decay time of 2 msec and the weight $w_{ii} = -100$ in Eqs. (7–8). Individual PSPs were modeled using the alpha function (Koch 1999) described as the difference of two exponentials with the rise time of 1 msec and the decay time of approximately 10 msec for excitatory and 20 msec for inhibitory neurons (Sayer et al. 1990). Since our simulations' time step was 1 msec, such PSPs were actually represented by a single-step jump followed by an exponential decay of 10 to 20 msec, as described by Eq. (8). The neuronal activity was simulated at 1 msec time step ignoring conduction delays, negligible for spatially compact neuronal circuits. Produced neuronal activity was downsampled at 100 Hz to simulate observations using a slow imaging technique such as calcium imaging, and then the observations dataset was formed by using the block-wise round-robin sampling described in Section 3.2. Table 3 aggregates the parameter definitions used in these simulations.

In either model, the connectivity matrix was estimated after simulating the observations data using a Matlab implementation of the EM algorithm as described in Appendix A. The EM sample size for the hidden neuronal population activities was taken as $M = 50$ for the weakly coupled cortical network model and $M = 150$ for the synfire model. Only the connectivity matrix weights were estimated, assuming that the PSP time constants were known. This was done to separate different sources of errors in the estimation, understanding that the focus here is on the shotgun connectivity inference. More generally, it is possible to set the PSP time constants using the average values available from physiological data without a significant impact on the estimation results, or such time constants can be estimated as a part of the EM procedure. For a more in depth discussion of this issue see (Mishchenko et al. 2011).

Table 3 The parameters of the realistic GLM cortical neuronal networks simulated in this paper

Number of neurons	50
Base firing rate ($\exp(b_i)$)	10 Hz
Actual average firing rate	10 Hz
Excitatory neurons	80 %
Inhibitory neurons	20 %
Connectivity sparseness	10 %
Simulation time step	1 msec
Max observation duration	3000 sec
Neurons per imaging block	20 %
Imaging strategy	block-wise round-robin
Excitatory PSP peak	Exp(0.5) mV
Inhibitory PSP peak	Exp(-2.3) mV
Excitatory PSP rise time	1 msec
Inhibitory PSP rise time	1 msec
Excitatory PSP decay time	$N_5(10, 2.5)$ msec
Inhibitory PSP decay time	$N_{10}(20, 5)$ msec
Refractory time	$N_1(2, 0.5)$ msec

Exp(λ) stands for the exponential probability distribution with mean λ and $N_p(\mu, \sigma)$ stands for the truncated-Normal probability distribution with mean μ, standard deviation σ, and lower bound p

All numerical experiments in this paper were performed on a 4 dual-core i7-processor desktop computer with 8GB of RAM memory. The numerical estimation problems could be generally solved in a reasonable amount of time on this workstation, however, we found that the necessity to keep up to M examples of the complete activity of the hidden neuronal populations in the EM algorithm imposed drastic requirements on the RAM usage. In particular, for the GLM cortical network model described here and using the said workstation, we were able to solve at most the models with $T = 3000$ seconds of neuronal activity observations and $M = 50$ examples of hidden activity. In this sense, the RAM amount in our hardware configuration set the limits on the numerical experimentation that was performed in this paper.

To set the parameter M, which defines the number of samples used to model the posterior distribution of hidden neuronal activities $P(Y|X; \mathcal{W})$, we tried different M such as $M = 10$, 50, 100 and 150. The value of $M = 50$ was the highest value that we could try on the above mentioned hardware configuration for the GLM neuronal networks. The value $M = 150$ was the highest that we could try for the synfire neuronal network. We found that $M = 10$ sufficed to obtain a solution, however, the noise in that solutions was high so that disconnected neurons frequently appeared as connected in the estimated connectivity matrices. $M = 50$ appeared to be sufficient to achieve satisfactory reconstructions of the weakly correlated cortical neuronal network

models but lacking in the case of the strongly correlated synfire model. M above 100 were sufficient to produce satisfactory results in the case of the synfire model as well.

3 Results

3.1 Correctness of the shotgun neuronal connectivity estimation

3.1.1 General results for the correctness of the shotgun neuronal connectivity estimation

One of the biggest challenges of the functional connectivity estimation in neuroscience remains the presence of unobserved or hidden inputs in neuronal population activity recordings. The shotgun connectivity estimation is a promising approach for alleviating this problem, suggesting to image large neuronal populations in small groups of random neurons and reconstructing the complete connectivity matrix from such partial observations.

In this section we demonstrate that the shotgun connectivity estimation can be guaranteed to allow recovering the complete neuronal connectivity matrix under rather general conditions. We assume that the activity of an observed neuronal population, $\mathcal{X}$, is modeled by a general parametric probability density $P(\mathcal{X}|\mathcal{W})$ with an "effective" connectivity matrix parameter $\mathcal{W}$. We will examine the properties of the maximum likelihood estimation (MLE) in the shotgun imaging. An estimator $\hat{\mathcal{W}}$ of a statistical model's parameter is said to be consistent if it converges in probability to the true parameter value as the size of the observations sample tends to infinity. It is known from the asymptotic estimation theory that the ML estimators are consistent whenever the model $P(\mathcal{X}|\mathcal{W})$ satisfies certain mild regularity conditions and the observations distribution $P(X|\mathcal{W})$ possesses no observation-indistinguishable parameter sets. The technical MLE regularity conditions require the compactness of the parameter space, the continuity of the model probability density, and the integrability of the log-likelihood functions. The condition of the absence of indistinguishable parameter sets, or the condition of the model's identifiability, requires that $P(X|\mathcal{W})$ is such that no two distinct neuronal activity models $\mathcal{W} \neq \mathcal{W}'$ can result in identical observations distributions $P(X|\mathcal{W}) \equiv P(X|\mathcal{W}')$.

It may be instructive to revisit the role that the identifiability condition plays in the consistency of the MLE. Let us consider a collection of observations of neuronal population activity $\{X^{(k)},\ k = 1, 2, \ldots, T\}$, such that can be obtained from repeated runs of an experiment or as different segments of one experiment. We will treat such observations as independent, with a caveat that will be more properly addressed in the Theorem 1 below. In the MLE, one aims to find the parameter value $\hat{\mathcal{W}}$ that maximizes the log-likelihood of the observations $\{X^{(k)}\}$. In the limit of large T, by the Law of Large Numbers, the average log-likelihood function of the observations $\{X^{(k)}\}$, $l(\hat{\mathcal{W}}|\{X^{(k)}\})$, will converge in probability to the expected log-likelihood function $l(\hat{\mathcal{W}}) = E[\log P(X|\hat{\mathcal{W}})]$,

$$\begin{aligned} l(\hat{\mathcal{W}}|\{X^{(k)}\}) &= \tfrac{1}{T}\sum_{k=1}^{k=T} \log P(X^{(k)}|\hat{\mathcal{W}}) \\ &\to E_{P(X|\mathcal{W})}[\log P(X|\hat{\mathcal{W}})], \end{aligned} \tag{13}$$

where the expectation value is with respect to the distribution $P(X|\mathcal{W})$ with the true parameter value $\mathcal{W}$. Gibbs inequality can then be used to demonstrate that $l(\hat{\mathcal{W}})$ achieves its global maximum if and only if $P(X|\hat{\mathcal{W}}) \equiv P(X|\mathcal{W})$ for all X, whereas by the identifiability condition this now implies $\hat{\mathcal{W}} = \mathcal{W}$. Under the technical conditions for the limit of maximum to equal the maximum of limit, one then can conclude that the sequence of the ML estimates $\hat{\mathcal{W}}_T = \arg\max l(\hat{\mathcal{W}}|\{X^{(k)}\})$ converges (in probability) to the true parameter value $\mathcal{W}$.

From the point of view of the connectivity estimation in incompletely observed neuronal populations, the hidden inputs problem arises in this view for no other reason that the identifiability condition becomes broken. That is, different models of hidden neuronal populations' connectivity can result in the same distribution of the observations. For instance, in the canonical example of the hidden inputs problem, where a direct connection is falsely identified between two observed neurons with a common input from a third "hidden" neuron, the error occurs because the correlated input to these neurons from the third unseen neuron exactly reproduces the activity that would be otherwise observed on these neurons if they were indeed connected. The violation of identifiability leads to multiple network models being able to reproduce the same empirical observations distribution $P(X|\mathcal{W})$ and, therefore, achieve the global maximum of log-likelihood (13). It is important to observe, however, that the true connectivity model $\mathcal{W}$ still maximizes log-likelihood (13) and so remains a ML solution. Therefore, it is not that hidden inputs somehow break the functional estimation of neuronal connectivity; in the presence of hidden inputs such estimation is simply not unique.

To examine this situation in the shotgun estimation, we initially recognize that the expected log-likelihood of the shotgun observations can be written as,

$$l(\hat{\mathcal{W}}) = E_S\left\{E_{P(X_S|\mathcal{W})}[\log P(X_S|\hat{\mathcal{W}})]\right\}, \tag{14}$$

where S is used here to label particular observed neuronal subpopulations and the external average is over all different such subpopulations imaged during a sparse neuronal activity imaging experiment. X_S refers to the part of the neuronal

population's activity observed on S and $P(X_S|\hat{\mathcal{W}})$ is the probability distribution of such activity given the connectivity model $\hat{\mathcal{W}}$. The inner average is over the true observations distribution $P(X_S|\mathcal{W})$.

Let us now use the above observation that the true connectivity matrix $\hat{\mathcal{W}} = \mathcal{W}$ is necessarily a global maximizer of Eq. (14). More significantly, $\hat{\mathcal{W}} = \mathcal{W}$ maximizes Eq. (14) by simultaneously maximizing all individual terms $E_{P(X_S|\mathcal{W})}[\log P(X_S|\hat{\mathcal{W}})]$, since evidently $P(X_S|\hat{\mathcal{W}}) = P(X_S|\mathcal{W})$ for all S whenever $\hat{\mathcal{W}} = \mathcal{W}$. Let us now ask whether there can exist another model $\mathcal{W}' \neq \mathcal{W}$ that can achieve the same maximum. Since $\hat{\mathcal{W}} = \mathcal{W}$ maximizes Eq. (14) by simultaneously globally maximizing all $E_{P(X_S|\mathcal{W})}[\log P(X_S|\hat{\mathcal{W}})]$, evidently any such alternative model must also simultaneously maximize all $E_{P(X_S|\mathcal{W})}[\log P(X_S|\hat{\mathcal{W}})]$. In turn, this implies that any such alternative maximizer $\mathcal{W}'$ must match the marginal distributions $P(X_S|\mathcal{W})$ on all S inspected in a sparse neuronal activity imaging experiment.

This leads us to the following conclusion: If a sparse neuronal activity imaging scheme covers a set of partial observations of a neuronal population's activity $P(X_S|\mathcal{W})$ with S in some collection $\mathbf{S} = \{S\}$, and if for any $\mathcal{W}' \neq \mathcal{W}$ there exist at least one S in $\mathbf{S}$ such that $P(X_S|\mathcal{W})$ and $P(X_S|\mathcal{W}')$ are not identically same, then the hidden inputs problem is unequivocally resolved by such an imaging arrangement and the complete connectivity $\mathcal{W}$ is uniquely identified by the collection of the observations $\{X_S, S \in \mathbf{S}\}$.

We state this proposition more formally bellow.

Definition 1 Let $P(\mathcal{X}|\mathcal{W})$ be a statistical model of neuronal population activity $\mathcal{X} = \{\mathcal{X}_t, t = 1, 2, \ldots\}$ such that $\mathcal{X}_t$ is a stationary stochastic process, and let $P(\mathcal{X}_{t:t+k}|\mathcal{W})$ be the stationary distribution of $k+1$-tuples $\mathcal{X}_{t:t+k} = \{\mathcal{X}_t, \mathcal{X}_{t+1}, \mathcal{X}_{t+2}, \ldots, \mathcal{X}_{t+k}\}$ from $P(\mathcal{X}|\mathcal{W})$. Let $\mathbf{S}$ be a set of $k+1$-tuples of neuronal subpopulations in the model $P(\mathcal{X}|\mathcal{W})$, $\mathbf{S} = \{S_{1:1+k}\}$, such that for any two different model parameters $\mathcal{W}$ and $\mathcal{W}'$ there exist at least one $S_{1:1+k}$ in $\mathbf{S}$ such that $P(X_{t:t+k|S_{1:1+k}}|\mathcal{W})$ and $P(X_{t:t+k|S_{1:1+k}}|\mathcal{W}')$ are not identically equal, where $X_{t:t+k|S_{1:1+k}}$ is the restriction of $\mathcal{X}_{t:t+k}$ to $S_{1:1+k}$. Then we say that the model $P(\mathcal{X}|\mathcal{W})$ is uniquely identified by the set of distributions $\mathbf{P}(\mathbf{S}) = \{P(X_{t:t+k|S_{1:1+k}}|\mathcal{W}), S_{1:1+k} \in \mathbf{S}\}$.

Note that, if the original model $P(\mathcal{X}|\mathcal{W})$ is not identifiable itself, then we will say that $\mathbf{P}(\mathbf{S})$ is uniquely identifying if it discriminates between all identifiable classes of the model $P(\mathcal{X}|\mathcal{W})$.

Definition 2 Assume that for any tuple of neuronal subpopulations $S_{1:1+k}$ in a set $\mathbf{S}$ there exist a tuple $S'_{1:1+k} \supset S_{1:1+k}$ in a different set $\mathbf{S}'$. Then we say that $\mathbf{S}'$ completely covers $\mathbf{S}$.

Theorem 1 *Let $P(\mathcal{X}|\mathcal{W})$ be a statistical model of neuronal population activity $\mathcal{X} = \{\mathcal{X}_t, t = 1, 2, \ldots\}$ and let $S = \{S_t, t = 1, 2, \ldots\}$, $S \sim P(S)$, be a series of partial observations of that model's activity over subpopulations of neurons S_t. Let $\mathcal{X}$ and S jointly define a stationary and ergodic stochastic process and assume that the classical MLE regularity conditions hold for the model $P(\mathcal{X}|\mathcal{W})$, namely:*

(A1) the parameter space $\mathcal{W} \in \mathfrak{W}$ is compact;

(A2) all distribution densities $P(\mathcal{X}_{t:t+k}|\mathcal{W})$ are continuous in $\mathcal{W}$;

(A3) $E\left[\left|\log P(X_{t:t+k|S_{t:t+k}}|\hat{\mathcal{W}})\right|\right] < \infty$ for all $\hat{\mathcal{W}}$ and $S_{t:t+k}$, where the expectation is over the stationary distribution $P(\mathcal{X}_{t:t+k}|\mathcal{W})$ for the true $\mathcal{W}$.

Assume further that the model $P(\mathcal{X}|\mathcal{W})$ is uniquely identified in the sense of Definition 1 by a set of distributions $\mathbf{P}(\mathbf{S}) = \{P(X_{t:t+k|S_{1:k+1}}|\mathcal{W}), S_{1:k+1} \in \mathbf{S}\}$ for some $\mathbf{S}$. Then, for any model of the partial observations $P(S)$ such that the support $\mathbf{S}' = \{S_{t:t+k} : P(S_{t:t+k}) > 0\}$ completely covers $\mathbf{S}$ in the sense of Definition 2, the ML estimator

$$\hat{\mathcal{W}}_T(\mathcal{X}, S) = \arg\max_{\hat{\mathcal{W}}} L(\hat{\mathcal{W}}|\mathcal{X}, S; T), \tag{15}$$

where

$$L(\hat{\mathcal{W}}|\mathcal{X}, S; T) = \sum_{t=1}^{t=T} \log P(X_{t:t+k|S_{t:t+k}}, S_{t:t+k}|\hat{\mathcal{W}}), \tag{16}$$

is consistent.

Proof The proof can be found in Appendix C. □

Theorem 1 makes use of the assumption that the stochastic process defined by the neuronal activities $\mathcal{X}_t$ together with the sequence of observations S_t is ergodic. Ergodicity of a stochastic process means that the averages over time can be substituted with the averages over the stationary distribution of that process. Namely, the basic Ergodic theorem asserts that

$$\lim_{T\to\infty} \frac{1}{T} \sum_{t=1}^{t=T} f(\theta^{t-1}\omega) = E_{P(\omega)}[f(\omega)], \tag{17}$$

where ω are the state sequence realizations from a stochastic process, θ is the operator of unit time-shift, and the expectation on the left is over the stationary distribution $P(\omega)$ (Varadhan 2001). Ergodicity is a basic property of many stochastic processes. In particularly important case of Markov processes, a Markov process is known to be ergodic whenever it possesses a unique stationary distribution (Bellet 2006).

Theorem 1 states that, if a sparse neuronal activity imaging protocol $\mathbf{S}'$ is able to inspect all neuronal subpopulations comprising an identifying set of the partial neuronal

activity distributions $\mathbf{P}(\mathbf{S})$ of a neuronal activity model $P(\mathcal{X}|\mathcal{W})$, then the MLE can be guaranteed to converge to the correct neuronal connectivity model $\mathcal{W}$, assuming the basic regularity conditions are met. Whenever the identifying set is covered during such an observation using either a non-deterministic or a reasonable deterministic protocol, the resulting neuronal connectivity inference problem can be thus said to possess the identifiability property, whereas in general identifiability given incomplete observations of a neuronal population is not guaranteed even if the original full neuronal population's activity model is identifiable.

A further observation is that the nature of the mapping from the identifying sets $\mathbf{P}(\mathbf{S})$ to the models $\mathcal{W}$ is not important, that is, it is not important by means of which statistics of $\mathbf{P}(\mathbf{S})$ the parameter $\mathcal{W}$ can be estimated and how. As long as such a mapping can be said to exist, the full model $\mathcal{W}$ is recoverable via the above MLE.

We formalize this latter observation in the form of the following corollary.

Corollary 1 *Let $T(\mathcal{X})$ be the sufficient statistics of a model of neuronal population activity $P(\mathcal{X}|\mathcal{W})$, and assume that $T(\mathcal{X})$ can be calculated from the set of stationary distributions $\mathbf{P}(\mathbf{S}) = \{P(X_{t:t+k}|_{S_{1:1+k}}|\mathcal{W}),\ S_{1:1+k} \in \mathbf{S}\}$. Then $\mathbf{P}(\mathbf{S})$ is uniquely identifying.*

Proof The statement follows from recognizing that for any two identifiable models $\mathcal{W} \neq \mathcal{W}'$ the respective sufficient statistics $T(\mathcal{X})$ have to be different. This implies that at least one distribution $P(X_{t:t+k}|_{S_{1:1+k}}|\mathcal{W})$ in $\mathbf{P}(\mathbf{S})$ necessarily has to be different for $\mathcal{W}$ and $\mathcal{W}'$ and, thus, $\mathbf{P}(\mathbf{S})$ is uniquely identifying. □

Theorem 1 shifts the burden of establishing the consistency of the shotgun estimation to the problem of finding uniquely identifying sets for different neuronal activity models. In general, uniquely identifying sets different from trivial one, that is, such comprising the complete observation $P(\mathcal{X}|\mathcal{W})$, do not exist. For certain linear and generalized linear models of neuronal population activity we obtain explicitly some uniquely identifying sets in Section 3.1.5. More generally, based on the inverse theorem of calculus, it may be expected that for general network models of neuronal activity parametrized by a $N \times N$ effective connectivity matrix $\mathcal{W}$ any set of N^2 linearly independent marginal distributions $P(X_S|\mathcal{W})$ will be sufficient to locally uniquely identify the complete connectivity matrix $\mathcal{W}$.

With regard to the former, consider a general probability density $P(\mathcal{X}|\mathcal{W})$ defined on a grid of d points in n dimensions. In this paragraph, we treat $P(\mathcal{X}|\mathcal{W})$ as a general parametric probability density that needs estimation, without necessarily making connections to any specific model of neuronal population activity. However, one can think of $P(\mathcal{X}|\mathcal{W})$ as the stationary distribution of $k+1$-tuples $\mathcal{X} = (\mathcal{X}_t, \mathcal{X}_{t+1}, \ldots, \mathcal{X}_{t+k})$ of the activity of N spiking neurons $\mathcal{X}_t = \{\mathcal{X}_{it}, i = 1, \ldots, N\}$, whereas then $d = 2^N$ and $n = k+1$, for example. In general, the above probability density contains $d^n - 1$ free parameters needed to specify the probabilities $P(\mathcal{X}|\mathcal{W})$ at each of the d^n points of the grid minus one normalization condition $\sum_{\mathcal{X}} P(\mathcal{X}|\mathcal{W}) = 1$. It is easy to see that all marginal distributions $P(X_S|\mathcal{W})$ of up to $n-1$ dimensions together provide $n(d-1) + n(n-1)/2!(d^2-1) + \ldots < (1+d)^n - d^n \approx nd^{n-1}$ linear constraints on $P(\mathcal{X}|\mathcal{W})$. One sees then that even specifying all marginal distributions together is insufficient to specify the above probability density uniquely, if $d > n$. Thus, the shotgun estimation can never be successful in that case—a complete observation of the model is required.

With regard to the latter, in practice the models of neuronal population activity are much more constrained and often are fully specified by a single connectivity matrix of N^2 elements, where N is the number of neurons in the model. Whenever two or more alternative models $\mathcal{W}$ can match the same observations distribution $P(X|\mathcal{W})$, this can happen in one of two ways: on a discrete set of observation-equivalent models $\{\mathcal{W}_1, \mathcal{W}_2, \ldots\}$ or on a continuous manifold of equivalent models $\mathfrak{W}$ containing the true model $\mathcal{W}$. The former would occur typically due to the presence of exact or approximate symmetries in the observations likelihood $P(X|\mathcal{W})$, and we will encounter an example of this situation in Section 3.1.2. The latter occurs whenever available observations are insufficient to uniquely constrain $\mathcal{W}$, that is, the estimation problem is underdetermined, and this situation is understood to correspond most directly to the classical problem of hidden inputs.

In the latter case one can argue, based on the inverse theorem of calculus, that it is only necessary to acquire N^2 linearly independent projections of the probability density $P(\mathcal{X}|\mathcal{W})$ to be able to (locally) uniquely constrain $\mathcal{W}$. For instance, let $T_k(\mathcal{X})$ be K statistics of a neuronal population activity model $P(\mathcal{X}|\mathcal{W})$, parametrized by a $N \times N$ connectivity matrix parameter $\mathcal{W}$. If $T_k(\mathcal{X}) \to t_k(\mathcal{W})$ uniformly as the sample size $T \to \infty$, then in the limit of large sample sizes one can expect to be able to reconstruct the complete connectivity matrix $\mathcal{W}$ by solving the system of nonlinear equations $t_k(\hat{\mathcal{W}}) = T_k(\mathcal{X})$. As is well known from calculus, such a solution is locally unique whenever the $K \times N^2$ Jacobian matrix $\mathcal{J} = (\delta t_k(\hat{\mathcal{W}})/\delta w_{ij})$ at the solution point is nonsingular. When one has $K = N^2$ linearly independent statistics available from the observations, such Jacobian becomes a square matrix and one can expect its determinant to be generally nonzero, thus providing for the local uniqueness of the solution $\hat{\mathcal{W}}$.

As a specific example, consider the set of all time-shifted correlations $(\Sigma_1)_{ij} = E[\mathcal{X}_{i,t+1}\mathcal{X}_{jt}]$. These clearly are functions of the model parameter $\mathcal{W}$. If the determinant

of the Jacobian $\mathcal{J} = (\delta(\Sigma_1(\mathcal{W}))_{ij}/\delta w_{i'j'})$ is nonzero, then one can expect the knowledge of Σ_1 to be sufficient to uniquely identify the complete connectivity matrix $\mathcal{W}$ at least locally. Here, $\mathcal{J}$ is a general $N^2 \times N^2$ matrix and, with the exception of certain specific circumstances such as the neuronal activity model having a structure specifically causing the degeneracy of $\mathcal{J}$ or $\mathcal{W}$ belonging to a set of Lebesgue measure zero, $\det \mathcal{J}$ can be expected to be nonzero and $\mathcal{J}$ to be nonsingular generally. Respectively, by Corollary 1 the set of all input-output distributions $P(\mathcal{X}_{i,t+1}, \mathcal{X}_{jt})$, providing the statistics Σ_1, would be sufficient for identifying $\mathcal{W}$ in such situations.

3.1.2 The shotgun connectivity estimation in the linear neuronal population activity model

In this section we perform a direct analysis of the shotgun connectivity estimation in the linear neuronal population activity models (3). We consider the input-output form of model (3) formulated for one continuously observed output neuron and a population of sparsely observed input neurons. We introduce a scalar output variable Z_{ik} and two vector input variables X_k and Y_k, representing the activities of the observed and the unobserved input neurons during different observations k, respectively, whereas Z_{ik} represents the activity of the output neuron i in an immediately following observation. These are related by

$$Z_{ik} = W_{iX_k} X_k + W_{iY_k} Y_k + \epsilon_{ik}, \tag{18}$$

where W_i is the row of the complete connectivity matrix $\mathcal{W}$ comprised of all input connection weights of the output neuron i, and W_{iX_k} and W_{iY_k} are the parts of W_i corresponding to the observed and the hidden inputs X_k and Y_k, respectively. ϵ_{ik} is an i.i.d. normal noise with zero mean and unit variance.

It should be made clear that here, unlike in model (3), we assume that the inputs X_k and Y_k are drawn i.i.d. from the stationary distribution of (3). This point is emphasized by our using in Eq. (18) a separate index k as opposed to the use of the time index t in Eq. (3). In other words, model (18) describes i.i.d. tuples (Z_{ik}, X_k, Y_k) distributed according to

$$P(Z_{ik}, X_k, Y_k) = P(Z_{ik}|X_k, Y_k; W_i) P(X_k, Y_k), \tag{19}$$

where $P(X_k, Y_k) = P(\mathcal{X}_k)$ is the stationary distribution of (3).

Model (3) and model (18) are related by the Ergodic theorem as long as the stochastic process (3) possesses a unique stationary distribution. In particular, one can see that the distribution (19) is exactly the stationary distribution $P(\mathcal{X}_{i,t+1}, \mathcal{X}_t)$ of the stochastic process defined by Eq. (3). We will show, therefore, that the complete connectivity matrix $\mathcal{W}$ in the model defined by Eq. (3) can be extracted from certain marginal distributions of $P(\mathcal{X}_{t+1}, \mathcal{X}_t)$ by using the MLE formulated for the model defined by Eq. (18).

The conditions under which the stationary distribution of the stochastic process (3) exists need to be stated. The existence of a unique stationary distribution of a continuous state-space Markov model can be guaranteed whenever the transition density $P(\mathcal{X}_{t+1}|\mathcal{X}_t; \mathcal{W})$ is continuous in $\mathcal{X}_{t+1}$ for all $\mathcal{X}_t$ and all trajectories $\mathcal{X}_t$ are bounded (Hairer 2010). In terms of the parameters of model (3), these translate into the requirements that the covariance matrix of the noise term ϵ_t is nonsingular and the absolute value-largest right eigenvalue of the matrix $\mathcal{W}$ is smaller in absolute value than 1. These requirements are not particularly restrictive. In particular, the latter is required for model (3) to be meaningful. Indeed, if $\mathcal{W}$ has a right eivenvalue greater in absolute value than 1 and the noise covariance matrix is nonsingular, then $\mathcal{X}_t$ exponentially diverges to infinity as $t \to \infty$ for all initial conditions, resulting in a clearly unacceptable behavior.

The stationary distribution $P(\mathcal{X}_k)$ is Gaussian (Rasmussen and Williams 2006) and can be parametrized by its mean and the covariance matrix Σ. By suitably offsetting $\mathcal{X}_k$, it is always possible to make the mean vanish, however, Σ cannot be generally reduced. Also, Σ satisfies the Lyapunov equation,

$$\Sigma = I + \mathcal{W}\Sigma\mathcal{W}^T. \tag{20}$$

Here, we ignore the latter equality and instead treat both the connectivity matrix $\mathcal{W}$ and the covariance matrix Σ as the free parameters of model (18). This has no real impact on the complexity of the calculations but allows producing more general results.

Below we state the two main results of this section.

Lemma 1 *The expected log-likelihood function of model (18) is*

$$\begin{aligned} l(\hat{W}_i, \hat{\Sigma}) = -1/2E \left\{ \frac{1 + W_i \Sigma W_i^T - 2\hat{W}_i \mathcal{A}_{X_k} W_i^T + \hat{W}_i \mathcal{A}'_{X_k} \hat{W}_i^T}{1 + B_{ik}^2} \right. \\ \left. + \log(1 + B_{ik}^2) \right\} \\ -1/2E \left\{ Tr[\Sigma_{X_k X_K} \hat{\Sigma}_{X_k X_k}^{-1}] + \log\det \hat{\Sigma}_{X_k X_k} \right\}, \end{aligned} \tag{21}$$

*where the subscript-notation in Σ refers to the blocks of Σ corresponding to the neuronal inputs identified by X_k and Y_k, with * referring to all row or column elements. B_{ik}^2, $\mathcal{A}_{X_k}$ and $\mathcal{A}'_{X_k}$ are*

$$\begin{aligned} \mathcal{A}_{X_k} &= \hat{\Sigma}_{*X_k} \hat{\Sigma}_{X_k X_k}^{-1} \Sigma_{X_k *} \\ \mathcal{A}'_{X_k} &= \hat{\Sigma}_{*X_k} \hat{\Sigma}_{X_k X_k}^{-1} \Sigma_{X_k X_k} \hat{\Sigma}_{X_k X_k}^{-1} \hat{\Sigma}_{X_k *} \\ B_{ik}^2 &= \hat{W}_i (\hat{\Sigma} - \hat{\Sigma}_{*X_k} \hat{\Sigma}_{X_k X_k}^{-1} \hat{\Sigma}_{X_k *}) \hat{W}_i^T \end{aligned} \tag{22}$$

W_i and Σ are the true connection weights and the covariance matrix, respectively, and the average is over all different subsets of observed neurons X_k.

Proof The proof can be found in Appendix C. □

Theorem 2 *Consider model (18) parametrized by a connectivity weights vector W_i and a nonsingular covariance matrix Σ defined on a compact parameter space $\Omega = \{(W_i, \Sigma)\}$. The sequence of the ML estimates of the parameters $(\hat{W}_i, \hat{\Sigma})$ in model (18) converges in probability in the limit of large numbers of observations $T_i \to \infty$ to the true values of W_i and Σ whenever the two sets of submatrices Σ_{*X_k} and $\Sigma_{X_kX_k}$ separately tile the entirety of the covariance matrix Σ.*

Proof Under the above assumptions, model (18) can be seen to satisfy the classical regularity conditions of the MLE, namely, the compactness of the parameter set, the continuity of the log-likelihood, and the dominance condition. Then, the sequence of the ML estimates for W_i and Σ converges in probability as the number of observations $T_i \to \infty$ to $\arg\max l(\hat{W}_i, \hat{\Sigma})$, where $l(\hat{W}_i, \hat{\Sigma})$ is given by Eq. (21). It can be verified by direct inspection that $\hat{W}_i = W_i$ and $\hat{\Sigma} = \Sigma$ achieve the global maximum of Eq. (21) by separately maximizing the expressions under both expectation values for all X_k. If the submatrices Σ_{*X_k} and $\Sigma_{X_kX_k}$ for sampled X_k cumulatively (but separately) tile the entirety of the matrix Σ, and moreover if Σ is nonsingular, then the solution of the optimality conditions $\Sigma_{X_k*}W_i = \Sigma_{X_kX_k}\hat{\Sigma}^{-1}_{X_kX_k}\hat{\Sigma}_{X_k*}\hat{W}_i$ and $\Sigma_{X_kX_k} = \hat{\Sigma}_{X_kX_k}$ for all X_k can be also seen to be unique, and so the above maximum is unique. □

Theorem 2 establishes the sufficient conditions for the consistency of the shotgun connectivity ML estimation in the linear neuronal activity model (3) under the conditions that the stationary distribution of model (3) exists and is unique.

We shall point out that the condition of tiling of Σ by Σ_{*X_k} and $\Sigma_{X_kX_k}$ can be restated also as the two conditions that the set of all observed input subsets $\{X_k\}$ cumulatively covers the range of all possible neuronal inputs $j = 1 \ldots N$ (equivalent to Σ_{*X_k} tiling Σ) and that the set of all $\{X_k \times X_k\}$ covers all possible same-time pairs of neuronal inputs $\{(j, j') : j, j' = 1 \ldots N\}$ (equivalent to $\Sigma_{X_kX_k}$ tiling Σ).

Also, we shall point out that the fact of the full coverage of Σ by the collections of Σ_{*X_k} and $\Sigma_{X_kX_k}$ is important for the recoverability of the complete connectivity matrix and not the manner in which such coverage is provided. That is, any organization of observations that provides such a coverage is equally capable of constraining the complete connectivity matrix $\mathcal{W}$. For instance, one plausible strategy for estimating $\mathcal{W}$ would be to image the activity of all neuronal pairs $(\mathcal{X}_{it}, \mathcal{X}_{jt})$ and $(\mathcal{X}_{i,t+1}, \mathcal{X}_{jt})$, one pair at a time, in any order.

Finally, we note that although Theorem 2 establishes that the global maximum of Eq. (21) is unique, under the specified conditions, the log-likelihood (21) can and does contain isolated local optima different from the global maximum. In particular, one finds a local "mirror" optimum at $\hat{\Sigma} = \Sigma$, $\hat{W}_i \approx -W_i$ in the limit of small fractions of observed inputs $p \to 0$, Fig. 1. The origin of this mirror optimum can be traced to the cancellation of the variations of the terms $(1 + B^2_{ik})^{-1}$ and $\log(1 + B^2_{ik})$, which dominate Eq. (21) in the limit $p \to 0$ and which are symmetric under $W_i \to -W_i$. The difference between expected log-likelihoods of the mirror and the true optima tends to zero as $O(p^2)$ as $p \to 0$.

3.1.3 The hidden inputs problem in the linear neuronal population activity model

In this section we produce an explicit example of the hidden inputs problem in the linear neuronal activity model, by taking advantage of $l(W_i, \Sigma)$ calculated in Section 3.1.2.

Let us consider a situation where the set of observed inputs X_t is kept constant throughout the experiment, $X_t \equiv X$. In that case, we can remove from Eq. (21) the expectation over different subsets of observed inputs X_t. Performing the variation with respect to $\hat{W}_{iX}$ then yields the following formula for $\hat{W}_{iX}$,

$$\hat{W}_{iX} = W_{iX} + W_{iY}\Sigma_{YX}\Sigma^{-1}_{XX} - \hat{W}_{iY}\hat{\Sigma}_{YX}\hat{\Sigma}^{-1}_{XX}. \tag{23}$$

From Eq. (23) it is easy to see that, if one has access to the input connection weights of the hidden neurons, $\hat{W}_{iY} = W_{iY}$, and the correct covariances, $\hat{\Sigma}_{XX} = \Sigma_{XX}$ and $\hat{\Sigma}_{YX} = \Sigma_{YX}$, then it is in fact possible to correctly estimate the connectivity weights W_{iX} even without observing the activity

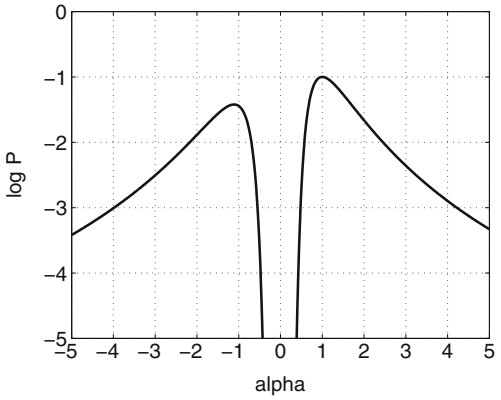

Fig. 1 An example of $l(\hat{W}_i, \hat{\Sigma})$ for a choice of W_i and $\Sigma = I$ along the solution ray $\hat{W}_i = \alpha W_i$, $\hat{\Sigma} = \Sigma$. The plot shows that $\alpha = 1$ is not a unique local maximum. The second "mirror" optimum is located at $\alpha \approx -1$

of any of the hidden neurons. At the same time, if the input connection weights of the hidden neurons or the correlations between the hidden and the observed neurons are ignored, for example, by setting $\hat{W}_{iY} = 0$ or $\hat{\Sigma}_{YX} = 0$, then the hidden inputs introduce a bias in the estimate of the observed neurons' connectivity that can be explicitly obtained as

$$E[\hat{W}_{iX} - W_{iX}] = W_{iY}\Sigma_{YX}\Sigma_{XX}^{-1}. \tag{24}$$

3.1.4 The error of the shotgun connectivity estimation in the linear neuronal population activity model

We can evaluate the posterior variance of the shotgun ML connectivity estimator in the linear neuronal population activity model (that is, the estimation error) by calculating the Laplace approximation in Eq. (21) around $\hat{W}_i = W_i$. Denoting $\hat{W}_i = W_i + \delta W_i$, we find with respect to δW_i,

$$l(\delta W_i) \approx -\frac{T_i}{2}\left\{1 + \delta W_i \frac{\mathcal{A}'}{1+B^2}\delta W_i^T\right\} + o(\delta W_i^2). \tag{25}$$

From Eq. (25), we then obtain the posterior variance of the ML estimator $\hat{W}_i$,

$$var(\hat{W}_i) = (1 + B^2)(\mathcal{A}' T_i)^{-1}. \tag{26}$$

For weakly correlated case, $\Sigma \approx I$, this can be reduced to a more intuitive expression,

$$var(\hat{W}_i) = \frac{1 + (1-p)|W_i|_2^2}{pT_i}, \tag{27}$$

where p is the fraction of the neurons contained on average in one observation X_t and $|W_i|_2$ is the 2-norm of the row-vector of the input connection weights W_i.

Equation (27) indicates that the posterior variance of the shotgun connectivity estimator grows proportionally to the square average of the connection weights and the number of neurons in the unobserved neuronal populations. The estimator's variance decreases inversely proportionally to the fraction of neurons contained in the observed input neuronal populations, p, and the total observation time of one neuron's output, T_i.

As we will see in Section 3, this result has a particularly simple interpretation: The error in the shotgun estimator $\hat{W}_i$ is introduced both by the intrinsic noise ϵ and the uncontrolled variability associated with the hidden inputs $\zeta_t = W_{iY_t}Y_t$. The reduction of that error for any given connection weight w_{ij} is achieved when the output of neuron i and the input of neuron j are observed together, which occurs in the total of pT_i observations. In particular, if both the output and the input neurons are observed randomly with probability p, per the original shotgun proposal, so that $T_i = pT$, then the shotgun estimator's error becomes respectively

$$var(\hat{W}_i) = \frac{1 + (1-p)|W_i|_2^2}{p^2 T} \text{ (original shotgun)}, \tag{28}$$

where T now is the total number of observations and p^2T is the number of the observations containing a given input-output neuronal pair.

3.1.5 The sufficient conditions for the correctness of the shotgun connectivity estimation in certain neuronal activity models

In this section we present certain explicit results for the correctness of the shotgun connectivity estimation in some neuronal activity models.

The theorem below asserts that under rather general conditions the set of triple-distributions $P(\mathcal{X}_{i,t+1}, \mathcal{X}_{jt}, \mathcal{X}_{kt})$ is uniquely identifying for the network models of neuronal activity when the number of neurons is large.

Theorem 3 *Consider a family of general "network type" Markov models of neuronal population activity characterized by a $N \times N$ connectivity matrix $\mathcal{W}$ and a transition probability density*

$$P(\mathcal{X}_t|\mathcal{X}_{t-1};\mathcal{W}) = \prod_{i=1}^{i=N} P(\mathcal{X}_{it}|W_i\mathcal{X}_{t-1}), \tag{29}$$

where W_i is the i^{th} row of $\mathcal{W}$ and $N = dim(\mathcal{X}_t)$. Let model (29) define an ergodic stochastic process and let $\log P(\mathcal{X}_t|\mathcal{X}_{t-1};\mathcal{W})$ be L_1 integrable under the stationary distribution of that process. Also, let $l_{T,N}(\mathcal{W}|\mathcal{X})$ be the average log-likelihood function for the realizations of the neuronal activity patterns $\mathcal{X} = \{\mathcal{X}_t, t = 1 \dots T\}$ in model (29),

$$l_{T,N}(\mathcal{W}|\mathcal{X}) = \frac{1}{NT}\sum_{t=1}^{t=T}\sum_{i=1}^{i=N} \log P(\mathcal{X}_{it}|\mathcal{X}_{t-1};\mathcal{W}). \tag{30}$$

In that case, if the sums

$$\mathcal{J}_{it} = \sum_{j=1}^{j=N} w_{ij}\mathcal{X}_{j,t-1} \to \mathcal{N}(m_i, \sigma_i^2) \tag{31}$$

in distribution as $N \to \infty$ for tuples $\mathcal{X}_{t-1}$ from $P(\mathcal{X}_{t-1})$ and some m_i and σ_i, possibly functions of N (the Central Limit Theorem), then the set of all triple-distributions $P(\mathcal{X}_{i,t+1}, \mathcal{X}_{jt}, \mathcal{X}_{kt})$ is uniquely identifying for model (29) in the limit $N \to \infty$ and, furthermore, $l_{T,N}(\mathcal{W}|\mathcal{X}) \to l_\infty(\mathcal{W})$ almost surely as $T, N \to \infty$, where

$$l_\infty(\mathcal{W}) = \frac{1}{N}\sum_{i=1}^{i=N}\int d\mathcal{X}_i d\mathcal{J}_i \frac{1}{(2\pi W_i\Sigma(\mathcal{X}_i)W_i^T)^{1/2}} \times \log P(\mathcal{X}_i|\mathcal{J}_i + W_i\mu(\mathcal{X}_i))e^{-\mathcal{J}_i^2/(2W_i\Sigma(\mathcal{X}_i)W_i^T)} \tag{32}$$

and $\mu(\mathcal{X}_i) = E[\mathcal{X}_t|\mathcal{X}_{i,t+1} = \mathcal{X}_i]$ and $\Sigma(\mathcal{X}_i) = cov(\mathcal{X}_t|\mathcal{X}_{i,t+1} = \mathcal{X}_i)$.

Proof The proof can be found in Appendix C. □

In Theorem 3, we directly require the validity of the Central Limit Theorem (CLT) for the sums $\mathcal{J}_{it}$. The CLT is seen to hold very widely in practice (Lehmann 1999). However,

the specific conditions for the validity of the CLT for sums of dependent random variables, such as the tuples $\mathcal{X}_t \sim P(\mathcal{X}_t)$, remain the subject of a very active research area and an extensive body of literature in statistics, for example, see (Berk 1973; Newman 1984; Doukhan 1994; Lehmann 1999; Coulon-Prieur and Doukhan 2000; Johnson 2001; Dedecker and Merlevede 2002; Bradley 2005; Davidson 2006; Klartag 2007; Guillotin-Plantard and Prieur 2010; Neumann 2013; Hall and Heyde 2014) and references therein. In practice, it may be the easiest to verify the CLT condition in Theorem 3 directly by checking that the shapes of $P(\mathcal{J}_{it})$ approach Gaussian. For instance, (Soudry et al. 2015) find that the CLT approximation works well in the exponential-GLM of spiking neuronal networks.

We can apply Theorem 3 to the case of the GLM of neuronal population activity. The GLMs of neuronal activity are of special interest in theoretical and computational neuroscience, see (Brillinger 1988; Chornoboy et al. 1988; Brillinger 1992; Plesser and Gerstner 2000; Paninski et al. 2004; Paninski 2004; Rigat et al. 2006; Truccolo et al. 2005; Nykamp 2007; Kulkarni and Paninski 2007; Pillow et al. 2008; Vidne et al. 2009; Stevenson et al. 2009). Below we state the two key results in that respect, which can be obtained by a direct application of Eq. (32).

Corollary 2 *Consider a family of generalized linear models of neuronal population activity* (6) *satisfying the conditions of Theorem 3. Then, the set of all distributions* $P(\mathcal{X}_{i,t+1}, \mathcal{X}_{jt}, \mathcal{X}_{kt})$ *is uniquely identifying in the limit* $N \to \infty$ *and*

$$\begin{aligned} &l_{T,N}(b, \mathcal{W}|\mathcal{X}) \to \\ &l_\infty(b, \mathcal{W}) = J_1(b, \mathcal{W}) - J_2(b, \mathcal{W}) \end{aligned} \tag{33}$$

almost surely, where

$$\begin{aligned} J_1(b, \mathcal{W}) = \frac{1}{N} \sum_i \mu_i \Bigg\{ &\frac{1}{(2\pi W_i \Sigma(i) W_i^T)^{\frac{1}{2}}} \times \\ &\int d\mathcal{J} \log f(\mathcal{J} + m_i') e^{-\mathcal{J}^2/(2W_i \Sigma(i) W_i^T)} \Bigg\} \end{aligned} \tag{34}$$

and

$$\begin{aligned} J_2(b, \mathcal{W}) = \frac{1}{N} \sum_i \Bigg\{ &\frac{1}{(2\pi W_i \Sigma W_i^T)^{\frac{1}{2}}} \times \\ &\int d\mathcal{J} f(\mathcal{J} + m_i) e^{-\mathcal{J}^2/(2W_i \Sigma W_i^T)} \Bigg\}. \end{aligned} \tag{35}$$

Here, $m_i = b_i + W_i \mu$, $m_i' = b_i + W_i \mu(i)$, $\mu = E[\mathcal{X}_t]$, $\mu(i) = E[\mathcal{X}_t | \mathcal{X}_{i,t+1} = 1]$, $\Sigma = cov(\mathcal{X}_t)$, *and* $\Sigma(i) = cov(\mathcal{X}_t | \mathcal{X}_{i,t+1} = 1)$.

Corollary 3 *Consider the conditions of Corollary 2 and let the neuronal activity model be the exponential-GLM with the nonlinearity function* $f(.) = \exp(.)$. *Then,*

$$J_1(b, \mathcal{W}) = \frac{1}{N}(\mu^T b + Tr[\mathcal{W} \Sigma_1^T]) \tag{36}$$

and

$$J_2(b, \mathcal{W}) = \frac{1}{N} \sum_i e^{b_i + W_i \mu + 2W_i \Sigma W_i^T}, \tag{37}$$

where $\mu = E[\mathcal{X}_t]$, $\Sigma_1 = E[\mathcal{X}_{t+1} \mathcal{X}_t^T]$ *and* $\Sigma = cov(\mathcal{X}_t)$, *and the uniquely identifying distributions are* $P(\mathcal{X}_{it}, \mathcal{X}_{jt})$ *together with* $P(\mathcal{X}_{i,t+1}, \mathcal{X}_{jt})$.

Note that in the exponential-GLM the special form of the log-likelihood allows one to relax the identifying set from all triple-distributions $P(\mathcal{X}_{i,t+1}, \mathcal{X}_{jt}, \mathcal{X}_{kt})$ to all pairwise same-time and input-output neuronal activity distributions $P(\mathcal{X}_{it}, \mathcal{X}_{jt})$ and $P(\mathcal{X}_{i,t+1}, \mathcal{X}_{jt})$.

Finally, for the linear model of neuronal activity (3) we have a similar result establishing that the identifying distributions are $P(\mathcal{X}_{it}, \mathcal{X}_{jt})$ and $P(\mathcal{X}_{i,t+1}, \mathcal{X}_{jt})$.

Theorem 4 *Consider the linear model of neuronal population activity* (3). *Assume that the stationary distribution of* (3) *exists and is unique. Furthermore, assume that the covariance matrix* $cov(\mathcal{X}_t)$ *is nonsingular. Then, the uniquely identifying distributions are* $P(\mathcal{X}_{it}, \mathcal{X}_{jt})$ *and* $P(\mathcal{X}_{i,t+1}, \mathcal{X}_{jt})$, *and*

$$\mathcal{W} = \Sigma_1 (\Sigma + \mu \mu^T)^{-1}, \tag{38}$$

where $\mu = E[\mathcal{X}_t]$, $\Sigma_1 = E[\mathcal{X}_{t+1} \mathcal{X}_t^T]$ *and* $\Sigma = cov(\mathcal{X}_t)$.

Proof Multiplying Eq. (3) on the left with $\mathcal{X}_t^T$ and averaging over time yields

$$\Sigma_1 = \mathcal{W}(\Sigma + \mu \mu^T), \tag{39}$$

where μ, Σ and Σ_1 are as defined above. By the assumptions of the theorem, the above expected values exist and are unique. If Σ is nonsingular, then one can multiply Eq. (39) on the right with $(\Sigma + \mu \mu^T)^{-1}$ to obtain

$$\mathcal{W} = \Sigma_1 (\Sigma + \mu \mu^T)^{-1}, \tag{40}$$

which establishes that μ, Σ and Σ_1 are the sufficient statistics. It then follows from Corollary 1 that $P(\mathcal{X}_{it}, \mathcal{X}_{jt})$ and $P(\mathcal{X}_{i,t+1}, \mathcal{X}_{jt})$ are uniquely identifying. □

Theorem 4 is clearly identical to the results of Section 3.1.2: providing all distributions $P(\mathcal{X}_{i,t+1}, \mathcal{X}_{jt})$ and $P(\mathcal{X}_{it}, \mathcal{X}_{jt})$ is equivalent to fully tiling Σ with the submatrices Σ_{*X_t} and $\Sigma_{X_t X_t}$. At the same time, supplementing Eq. (40) with Eq. (20) allows one to show that Σ_1 itself is in fact sufficient to uniquely constrain $\mathcal{W}$ at least locally, by solving Eq. (20) for $\Sigma(\mathcal{W})$ first and then Eq. (40) for $\mathcal{W}(\Sigma_1)$. This is in line with the general discussion in the end of Section 3.1.1.

3.1.6 More efficient parameter estimation in the shotgun approach in certain neuronal activity models

Theorems 2, 3 and 4 can be used to offer an advantageous way for calculating the parameters of linear and generalized linear neuronal activity models in the shotgun-type neuronal activity imaging experiments. Specifically, if the statistics $\mu = E[\mathcal{X}_t]$, $\Sigma = cov(\mathcal{X}_t)$ and $\Sigma_1 = E[\mathcal{X}_{t+1}\mathcal{X}_t^T]$ can be obtained from observations, then one can directly use Theorem 4 to find, for instance,

$$\hat{\mathcal{W}} = \Sigma_1(\Sigma + \mu\mu^T)^{-1} \tag{41}$$

for the connectivity parameter $\mathcal{W}$ of a linear model of neuronal activity. These statistics can be obtained from observations efficiently and used to perform the estimation from data of very large size as well as in online manner.

For the exponential-GLM, we can make use of Eq. (36) and Eq. (37) in Theorem 3 to obtain

$$(\hat{b}, \hat{\mathcal{W}}) = \arg\max_{b,\mathcal{W}} \left(\mu^T b + Tr[\mathcal{W}\Sigma_1^T] - \sum_i e^{b_i + W_i\mu + 2W_i\Sigma W_i^T} \right). \tag{42}$$

For the GLM of neuronal activity with general nonlinearity, we obtain from Theorem 2

$$(\hat{b}, \hat{\mathcal{W}}) = \arg\max_{b,\mathcal{W}} \left(J_1(b, \mathcal{W}) - J_2(b, \mathcal{W}) \right), \tag{43}$$

where J_1 and J_2 are defined by Eq. (34) and Eq. (35), respectively.

3.2 Alternative organizations of the shotgun neuronal population activity imaging

The results obtained in Section 3.1 have important implications for the question of the design of the shotgun neuronal activity imaging experiments. In particular we see that, to be able to reconstruct a complete neuronal connectivity matrix, it is only important that the identifying set $\mathbf{P}(\mathbf{S})$ is covered by the observations, and the manner in which such coverage is provided is not important. Moreover, per general discussion in Section 3.1.1, one may expect that the imaging of all input-output neuronal pairs in a neuronal network may be generally sufficient to uniquely identify the connectivity matrix of complete neuronal populations. Alternatively, Section 3.1.5 provides specific conditions that can be guaranteed to allow the identification of complete neuronal connectivity matrices in several general settings.

These results imply that alternative organizations of the shotgun neuronal activity imaging can be introduced that can be more advantageous for experimental settings.

A particularly advantageous and conceptually simple one such organization of neuronal activity imaging is the block-wise round-robin sampling, illustrated in Fig. 2. In this approach, a neuronal population is imaged using a sequence of contiguous blocks. Each pair of input and output blocks is imaged for a set period of time T_b. The blocks are then moved through the population so that all possible combinations of input and output blocks are inspected throughout the complete experiment.

The key advantage of the block-wise round-robin strategy is that it can be easily implemented by using already existing calcium imaging tools, by scanning two confocal or two-photon microscopes over a large population of neurons. Another advantage of this strategy is computationally simpler problem of the connectivity estimation, compared to that obtained for fully random sampling such as used in (Turaga et al. 2013; Keshri et al. 2013).

The block-wise round-robin sampling strategy with two scanning blocks is suitable for collecting all input-output and same-time pairs of neuronal activities $(\mathcal{X}_{i,t+1}, \mathcal{X}_{jt})$ and $(\mathcal{X}_{it}, \mathcal{X}_{jt})$, respectively, which per the discussion above can guarantee correct estimation of the connectivity matrix in the linear and the exponential generalized linear models of neuronal activity. The block-wise round-robin sampling strategy with larger number of blocks can be used to collect the triple-correlations $(\mathcal{X}_{i,t+1}, \mathcal{X}_{jt}, \mathcal{X}_{kt})$.

3.3 The impact of the missing data on the connectivity estimation

In Section 3.1.4 we calculated the error of the shotgun connectivity estimator in the linear neuronal activity model. It is interesting now to return to these results from a somewhat different perspective.

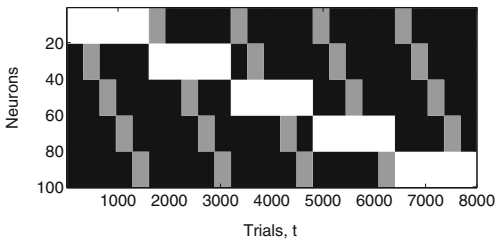

Fig. 2 Block-wise round-robin neuronal population activity imaging strategy. In this strategy, the neuronal population is imaged as a sequence of contiguous blocks of input and output neurons. During one section of the experiment, the neurons in one input and one output block are observed simultaneously for a fixed time T_b. All possible combinations of input and output blocks are observed during the entire experiment. This figure illustrates the block-wise round-robin sampling strategy applied to a hypothetical population of 100 neurons with 20 neurons observed in each input and output block. White color indicates the neurons in the output blocks and gray color indicates the neurons in the input blocks. In each observation, the activity of all marked neurons should be observed simultaneously

In particular, let us consider a segment of a block-wise round-robin neuronal activity imaging experiment with a fixed input and output observation blocks. We can relate the activity of the neurons in the observed input and output blocks as

$$Z_t = f(\mathcal{W}_{ZX} X_t + \zeta_t + \epsilon_t), \tag{44}$$

where Z_t is the column-vector of the activities of the neurons in the output block, X_t is the column-vector of the activities of the neurons in the input block, and we introduced a new random variable $\zeta = \mathcal{W}_{ZY} Y$, which represents the combined input of the hidden neurons into the observed neuronal outputs. The notation $f(.)$ alludes generally to the presence of a functional relationship between Z_t, X_t and $\zeta_t = \mathcal{W}_{ZY} Y_t$, such as described by Eqs. (3) or (6). For the qualitative discussion below the specific form of that relationship is not essential, and thus, we do not specify it more definitely below.

Posed from this perspective, the shotgun connectivity estimation appears now as the problem of estimating the blocks of connectivity matrix $\mathcal{W}_{ZX}$ given the observations of the activity of the respective input and output neurons X and Z, whereas the unobserved neurons enter the estimation in the form of only the additional noise ζ. The noise ζ is structured and correlated with X, which introduces both a variance and a bias in the estimates $\hat{\mathcal{W}}_{ZX}$. The knowledge of the structure of ζ can be used to remove the bias from $\hat{\mathcal{W}}_{ZX}$ (see Section 3.1.3 for an example). However, the additional statistical uncertainty introduced by ζ cannot be removed other than by increasing the sample size. We can roughly estimate that added uncertainty by approximating the variance of ζ as $var(\zeta) = var(\mathcal{W}_{ZY} Y) \approx |\mathcal{W}_{ZY}|^2 var(Y)$, and then

$$\begin{aligned} var(\hat{\mathcal{W}}_{ZX}) &\propto (T_b var(X))^{-1} var(\epsilon + \zeta) \\ &\approx (T_b var(X))^{-1} (var(\epsilon) + |\mathcal{W}_{ZY}|^2 var(Y)), \end{aligned} \tag{45}$$

where $|\mathcal{W}_{ZY}|^2$ is understood to be the average 2-norm of the rows of $\mathcal{W}_{ZY}$ and $var(X)$ and $var(Y)$ are the typical variances associated with the variables X_{it} and Y_{it}. In the limit where the size of the hidden neuronal population is large, we can further write

$$var(\hat{\mathcal{W}}_{ZX}) \propto s N_h A_w^2 / T_b, \tag{46}$$

where N_h is the number of neurons in the typical unobserved neuronal population, A_w is the root mean square average of the (nonzero) neuronal connectivity weights, s is the sparsity of the connectivity matrix, and T_b is the number of observations containing a given input-output neuronal pair.

Clearly, Eq. (46) is similar to Eq. (28) in Section 3.1.4. Eq. (46) provides a useful qualitative estimate for the errors of the shotgun connectivity estimation in general settings. We see that the primary source of that error is the uncontrolled fluctuations in the activity of the observed neuronal

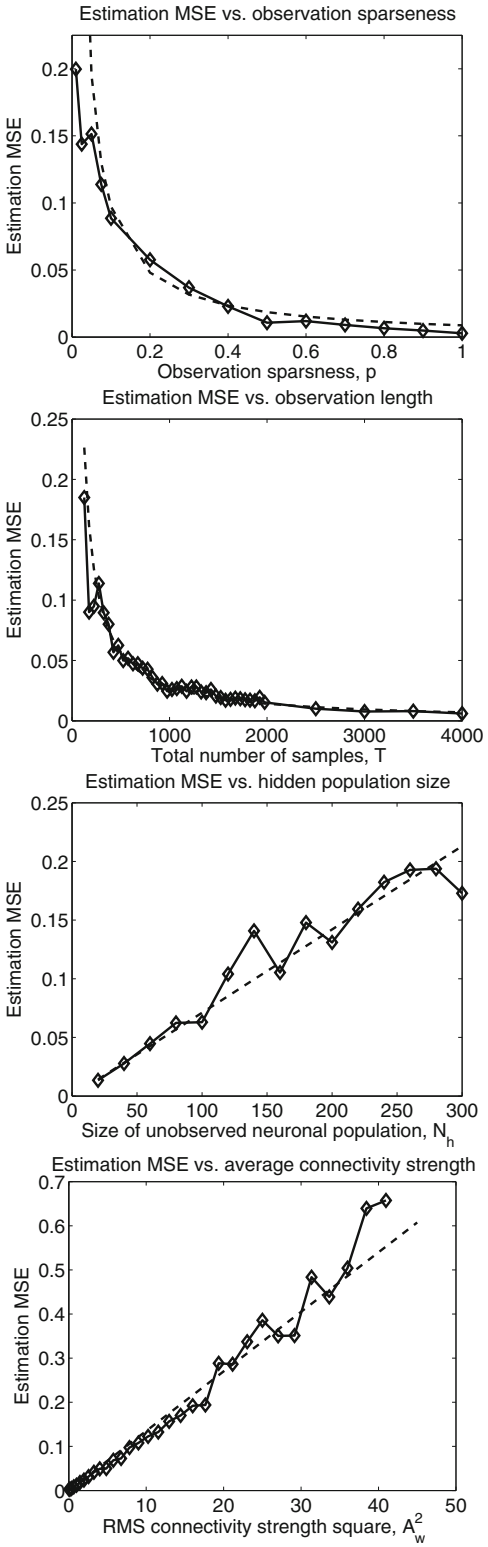

Fig. 3 The properties of the shotgun connectivity estimation in relation to the missing data. From top to bottom, the posterior error of the shotgun estimator is shown in relation to the observations' sparseness, the total number of observations, the size of hidden populations, and the rms average connectivity strength. The results of numerical simulations are shown with solid line and dashed lines show the theoretical predictions using Eq. (46). The simulation parameters are described in Table 1

populations produced by the input from hidden neurons. Such fluctuations grow with the connectivity strength, sA_w^2, and the size of hidden neuronal populations, N_h. The impact of those fluctuations is reduced via collecting more observations of given input-output neuronal pairs as T_b^{-1}.

We use Eq. (46) to illustrate the qualitative dependence of the connectivity estimation errors in the shotgun estimation on the size of hidden populations, typical strength of neuronal connectivity, the number of observations, and the sparseness of observed neuronal populations. Figure 3 shows these predictions together with the results of direct numerical simulations of the shotgun connectivity estimation in linear neuronal activity models, Section 2.4.1.

3.4 Numerical simulations of the shotgun connectivity estimation in realistic neuronal network models

In this section we perform numerical simulations of neuronal connectivity estimation from partially observed neuronal populations in realistic GLMs of cortical neuronal networks activity.

As the first case study here, we examine the shotgun connectivity estimation in a small model of $N = 10$ neuron synfire network, shown in Fig. 4. Synfire networks present one of the worst examples of the hidden inputs problem, where the correlations can propagate over large distances and emulate strong connections between very remote neurons.

We first inspect the scenario where a fixed population of 5 neurons is being continuously imaged, as indicated in Fig. 4 by solid circles. This scenario corresponds to the typical neuroimaging situation in which a fixed population of neurons is continuously observed while the rest of neurons are not observed. As a measure used to estimate the connectivity we use the time-shifted correlogram of lag 1 bin, widely employed in functional connectivity literature, and the direct GLM estimation following (Mishchenko et al. 2011). The results of these simulations are shown in Fig. 5. One can see that either the correlogram and the GLM estimation in this scenario produce strong spurious connections, namely, such seen between the neurons 4 and 9, 6 and 3, 9 and 6, etc.

We then simulate the connectivity matrix estimation in the same model using the block-wise round-robin imaging

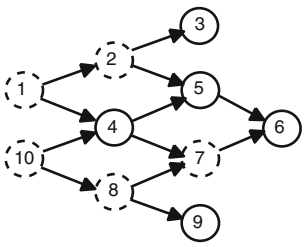

Fig. 4 The layout of the model synfire neuronal network used in the simulations in this paper

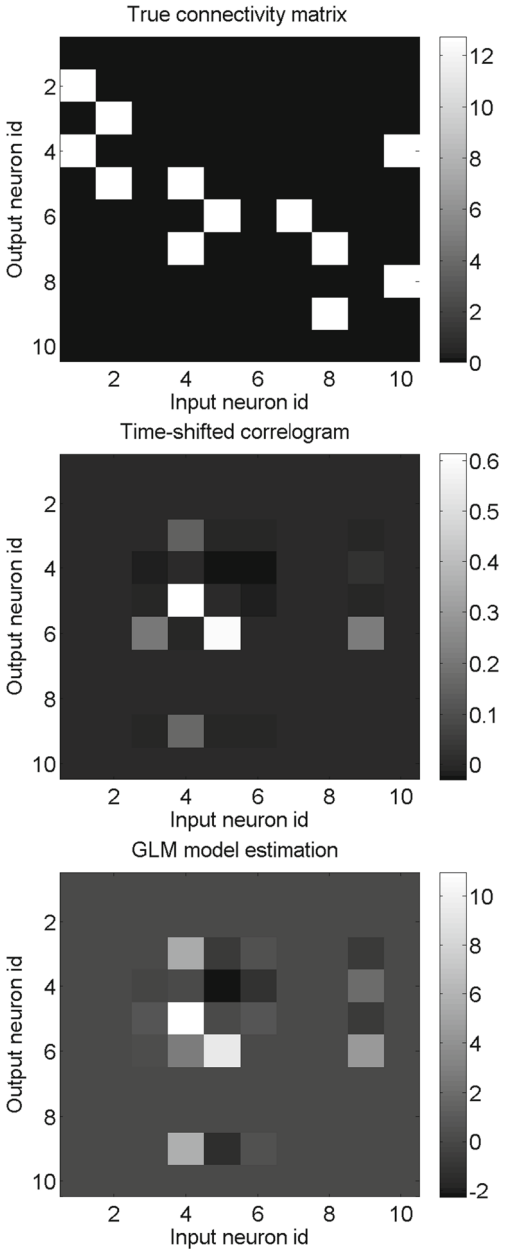

Fig. 5 The hidden inputs problem in the model synfire network in Fig. 4. The top panel shows the true connectivity matrix for the circuit. The middle panel shows the connectivity matrix estimation result using the time-shifted correlogram calculated for the population of neurons indicated in Fig. 4 with solid circles and $T = 10$ seconds of neuronal activity data. The bottom panel shows the GLM estimation of the same connectivity matrix performed under the same conditions. The simulation parameters are described in Table 2

strategy of Section 3.2, with the block size of 2 neurons, and the numerical EM connectivity matrix estimation algorithm of Section 2.3. The results of these simulations are shown in Fig. 6. Despite the fact that at most 4 neurons are observed in this scenario at any given time, the complete connectivity matrix is indeed recovered well. The strength of the false-positive connections between the neurons 4-9, 6-3 and 9-6

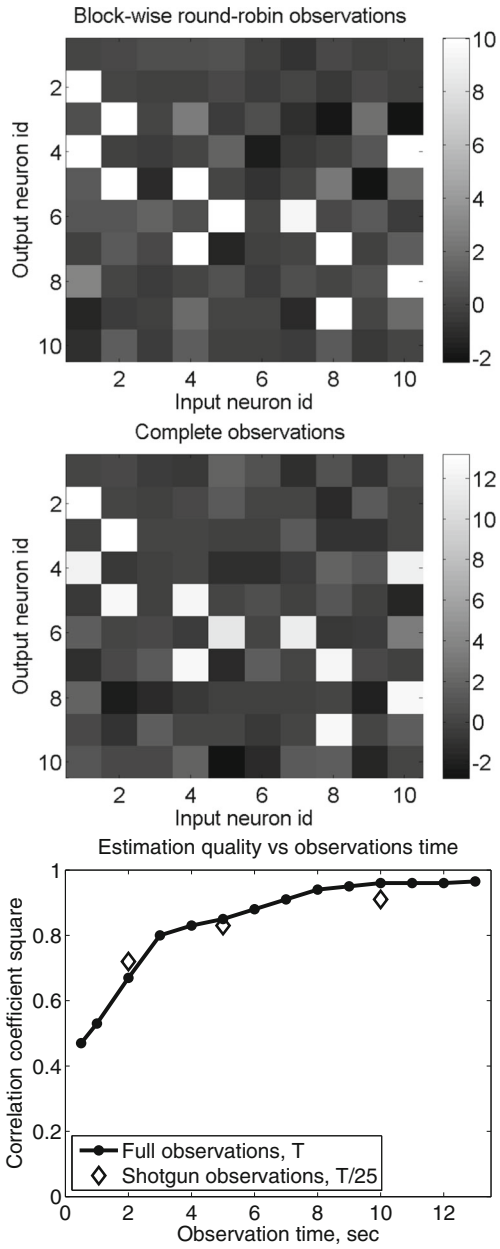

Fig. 6 Estimation of the complete connectivity matrix in the model synfire network in Fig. 4 using the block-wise round-robin sparse neuronal activity imaging. The top panel shows the result of the connectivity matrix estimation using this approach and $T = 50$ seconds of neuronal activity data. The middle panel shows, for comparison, a similar reconstruction using the complete observation and $T = 10$ seconds of neuronal activity. The bottom panel compares the quality of the connectivity matrix reconstruction for the block-wise round-robin imaging (diamonds) and the complete observation (solid line). The block-wise round-robin imaging points are shown at the "equivalent" times calculated as $T' = p^2T$, see main text. The simulation parameters are described in Table 2

is reduced by a factor of 2 to 3 as compared to Fig. 5. At the same time, the reconstructions obtained are substantially more noisy and require significantly more observations to suppress additional noise, as compared to such obtained from the observation of the complete neuronal population for the same duration of time. We observe that the accuracy of the shotgun connectivity estimation with the observation time T in these simulations is comparable to that using the complete observation and the imaging time p^2T, the bottom panel in Fig. 6. This is in general agreement with the results of Section 3.3.

Finally, we use our algorithms to perform the simulations of the shotgun connectivity estimation in a realistic model of weakly coupled cortical neuronal networks of $N = 50$ neurons. The results of these simulations are shown in Fig. 7. We again are able to recover the complete connectivity matrix from partial observations of neuronal population activity. Once again, the data size necessary to achieve a

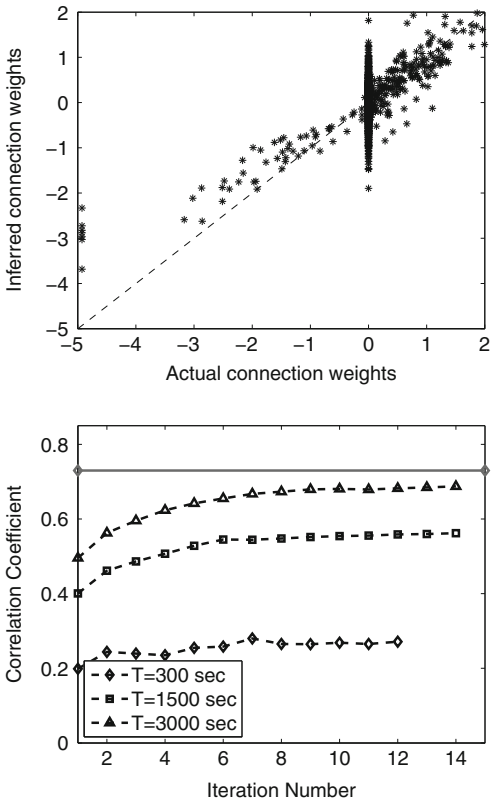

Fig. 7 The shotgun connectivity estimation in a model of a realistic weakly coupled cortical neuronal network. The upper panel shows the result of the reconstruction of the complete connectivity matrix in such a model using $p = 0.2$ block-wise round-robin sparse neuronal activity imaging and $T = 3000$ seconds of observation data. The multiplicative bias seen in the reconstructed weights is the finite time-discretization bias discussed in (Mishchenko et al. 2011) (not corrected here). The reconstructed connection weights reproduce the true connection weights well. However, the reconstructed connectivity matrices are more noisy. The bottom panel shows the correlation coefficient of the reconstructed and true connection weights as a function of the EM algorithm's iteration number, for $T = 300$, $T = 1500$, and $T = 3000$ seconds of total observation time. Solid gray line represents the baseline reconstruction obtained in the same model using the complete observation dataset and $T = 60$ seconds of neuronal activity. The simulation parameters are described in Table 3

given accuracy is significantly increased when using sparse observations as compared to that obtained when observing the complete neuronal population. Specifically, if good connectivity reconstructions are obtained in our simulations with the entire network observed from a total of $T = 60$ seconds of neuronal activity, in the simulations with $p = 20$ % block-wise round-robin imaging the total observation time needed to achieve similar reconstructions' accuracy approached $T = 3000$ seconds, the lower panel in Fig. 7.

4 Discussion and conclusions

The shotgun sampling solution of the common inputs problem is a promising approach for functional estimation of neuronal connectivity in large neuronal networks in the brain without requiring the simultaneous imaging of entire neuronal populations. By statistically estimating the neuronal connectivity from a collection of partial observations of different neuronal sub-populations' activity patterns, the shotgun sampling offers a possibility of recovering the connectivity matrix in realistically large neuronal circuits by using existing limited imaging resources.

In this paper, we establish analytically and in simulations certain important properties of such shotgun neuronal connectivity estimation.

In Theorem 1 of Section 3.1.1 we determine the sufficient conditions for the recovery of the complete connectivity matrices of large neuronal populations to be possible from shotgun-like sparse neuronal activity imaging. In Sections 3.1.2, 3.1.3 and 3.1.4 we examine more closely the shotgun connectivity estimation in linear models of neuronal population activity and derive analytically the observations' log-likelihood, the maximum likelihood estimator, and certain key properties of that estimator. In Section 3.1.5, we present explicit sufficient conditions for the correctness of the shotgun connectivity estimation in certain linear and generalized linear neuronal activity models, where the neuronal firing rates can be described as a general nonlinear function of linearly summed inputs. These cover a great variety of practically interesting network models of neuronal activity. In particular, we show that the same-time and time-shifted covariance matrices $E[\mathcal{X}_t\mathcal{X}_t^T]$ and $E[\mathcal{X}_{t+1}\mathcal{X}_t^T]$ are sufficient in linear and exponential generalized linear models of neuronal activity to uniquely identify the complete connectivity matrix. In general GLM of neuronal activity, we find that the observation of all triples $(\mathcal{X}_{i,t+1}, \mathcal{X}_{jt}, \mathcal{X}_{kt})$ is sufficient for the recovery of the complete connectivity matrix.

We find that the shotgun observations' log-likelihood can have multiple local maxima even when the MLE in the original neuronal activity model is free of spurious local solutions. In particular, in the linear neuronal activity model where the MLE in full-observations case is globally and locally unique, we show in Section 3.1.2 that two local maxima exist in the shotgun imaging setting—the true solution $\hat{\mathcal{W}}_{true} = \mathcal{W}$ and the "mirror" solution $\hat{\mathcal{W}}_{mirror} \approx -\mathcal{W}$. This property of the shotgun imaging MLE can pose difficulties for iterative ML algorithms such as the Expectation Maximization algorithm. Simple heuristics may be able to help avoid the mirror optimum-like solutions in practice. For example, one can decide to inspect the "mirror" solution likelihoods for all candidate ML solutions $\hat{\mathcal{W}}$. This strategy, however, may not be plausible if the fraction of observed neurons p is small, as the difference between the likelihoods of the true and the mirror solutions may quickly approach zero in that setting. Alternative resolution of the mirror-optima problem can be based on the use of a-priori information. Such a-priori information may include the excitatory or inhibitory identity of one or several neurons in the population or the relative abundances of the excitatory and inhibitory neurons, which may be rather easy to estimate beforehand. By requiring given neurons in the reconstruction to be excitatory or by requiring a particular split between the abundances of excitatory and inhibitory neurons the sign of the solution can be fixed.

We find that the lack of complete observability of neuronal populations in the shotgun-like activity imaging leads to an increase in the statistical error of the associated connectivity estimator, warranting the necessity of a respective increase in the imaging time in order to suppress that error. We find that the minimum shotgun imaging data size needs to increase proportionally to the number of neurons in the unobserved neuronal populations as well as the square-average of the neuronal connection weights. Furthermore, the data size needs to increase as the inverse square of the average fraction of neurons covered by a single observation. These scalings are inopportune for the reconstructions of neuronal connectivity, if the fraction of observed neurons needs to remain small.

Theorem 1 of Section 3.1.1 has important implications for the design of alternative shotgun-like sparse neuronal activity imaging experiments. In particular, it establishes that any sparse neuronal activity imaging scheme that covers a particular set of "identifying" neuronal activity distributions will be sufficient for the recovery of the complete connectivity matrix in a neuronal population. It is not important how or in what manner such coverage is provided, it is important only that such coverage is complete. This result allows for designing alternative shotgun-like sparse neuronal activity sampling protocols optimized for different experimental conditions.

Taking advantage of this result, in Section 3.2 we propose experimentally particularly advantageous alternative

organization of the shotgun neuronal activity imaging in the form of multi-block scanning of neuronal populations' activity. In this approach, the neurons are imaged sequentially in two or more contiguous blocks of "input" and "output" neurons, whereas all possible combinations of input and output blocks are observed throughout the experiment. This experiment design guarantees the coverage of all same-time and time-shifted neuronal activity pairs—necessary for the reconstruction of complete connectivity matrix in linear and exponential linear neuronal activity models—and has further advantage of allowing straightforward implementation using existing calcium imaging tools, as well as a simpler numerical connectivity estimation. We hope that the conceptual simplicity and the possibility of straightforward implementation will allow the "block-wise round-robin" sparse neuronal activity imaging to be realized experimentally in near future.

Another important issue raised by this study is the development of scalable approaches for numerical connectivity estimation in shotgun-like imaging setting. We demonstrated here the shotgun connectivity estimation in model neuronal populations with up to $N = 50$ neurons. In practice, the reconstructions of real neuronal circuits will require solving the same computational problem for thousands if not millions of neurons. The SMC EM procedure proposed in this work for general shotgun estimation is efficient, requiring $O(N^2M^2T)$ time for the E-step and $O(N^2MT)$ time for the M-step, as well as parallelizable, making the solution of the above problems possible on high-performance computing infrastructures already existing around the world. Faster sampling schemes for hidden neuronal populations' activity may be also investigated, for example, such as the fast Metropolis-Hastings algorithm proposed in (Mishchenko and Paninski 2011), which can reduce the cost of the E-step to $O(N^2MT)$.

The requirement to remember up to M examples of the entire hidden neuronal population's activity was the most significant burden on the numerical SMC EM algorithm in this work. For instance, for $N = 10^4$ neurons, $M = 100$ EM samples and $T = 10^4$ seconds of neuronal activity recorded at 100 Hz, the sample of the hidden neuronal activities constitutes staggering 10^{12} neuronal activity states. While this problem can be solved by partitioning the data over the nodes of a supercomputing infrastructure, the search of alternative approaches for reducing the memory footprint of the shotgun EM connectivity estimation is of interest.

Among the possible solutions to this problem is the use of alternative imaging schemes, such as the block-wise round-robin strategy described above, where the estimation of the connectivity matrix can be performed in blocks, whereas only one block of the connectivity matrix corresponding to the given input and output neurons observed over certain period of time needs to be considered. While not affecting N or M, this reduces T to at most such containing the observations involving the given input and output neuronal blocks.

Another interesting idea is to use approximate models of the hidden neuronal populations' input. For example, one can try to model the combined input of hidden neurons to observed neurons by using a multivariate Gaussian distribution, constructed based on the current estimate of the connectivity between the hidden and the observed neurons or by some other means. In that case, the storage of the state of all the samples of the entire hidden neuronal populations' activity will not be necessary.

Finally, a very promising option is to make use of the sufficient statistics of the connectivity estimation problem for a given neuronal activity model, such as obtained in Section 3.1.6. This allows using smaller sets of sufficient statistics in place of directly large hidden neuronal population activity samples. We provide the formulas necessary to implement that approach for certain neuronal activity models in Section 3.1.6. For exponential GLM, this idea had been successfully implemented in (Soudry et al. 2015).

Our work leaves several questions open for further investigation. Among these is the question of finding the identifying sets of general neuronal population activity models and, in particular, of the possibility to uniquely identify any network-like model of neuronal activity by just input-output pairwise distributions $P(\mathcal{X}_{i,t+1}, \mathcal{X}_{jt})$. Another set of questions is related to the alternative designs of sparse neuronal activity imaging experiments: What are other experimentally interesting sparse neuronal activity imaging strategies? Do different sparse imaging strategies offer different speed of convergence of the neuronal connectivity estimation? What are the important properties of alternative sparse imaging strategies? We hope that our results will stimulate further research into these topics as well as facilitate experimental realization of the sparse neuronal activity imaging and connectivity inference in model organisms.

Acknowledgments The author acknowledges the financial support via the TUBITAK ARDEB 1001 research grant number 113E611 (Turkey) and Bilim Akademisi—The Science Academy (Turkey) Young Investigator Award under BAGEP program. The author acknowledges a key discussion with Liam Paninski leading to this work, and Daniel Soudry's comments on an early version of this manuscript. The author is also thankful to the anonymous reviewers, whose comments led to many critical improvements of the manuscript.

Compliance with Ethical Standards

Conflict of interests The author declares that he has no conflict of interest.

Appendix A: Sequential Monte Carlo Expectation Maximization algorithm for the numerical solution of the shotgun connectivity estimation problem in general Markov models of neuronal population activity

The EM algorithm (Dempster et al. 1977) is the standard method of statistical inference in the presence of missing data. Briefly, the EM algorithm produces at least a locally maximum likelihood estimate of the parameters of a model $P(X, Y|\theta)$ given a set of observations X with the data Y missing, $\hat{\theta} = arg\max \sum_Y P(\theta, Y|X)$. The EM algorithm produces a sequence of parameter estimates $\hat{\theta}^q$ by iteratively maximizing the functions $Q(\theta|\hat{\theta}^q)$,

$$Q(\theta|\hat{\theta}^q) = E_{P(Y|X,\hat{\theta}^q)}[\log P(X, Y, \theta)], \tag{47}$$

where $Q(\theta|\hat{\theta}^q)$ at each step is calculated by constructing M samples of the unavailable data Y from $P(Y|X, \hat{\theta}^q)$ and using the following average,

$$Q(\theta|\hat{\theta}) = \frac{1}{M}\sum_{k=1}^{M} \log P(X, Y^k, \theta). \tag{48}$$

In the case of the shotgun sampling, the sampling step of the EM algorithm can be implemented using the forward-backward algorithm (Rabiner 1989) and the sequential Monte-Carlo method also known as the Particle Filtering (Godsill et al. 2001). In this case, the distribution of the hidden neuronal activities at every observation is modeled by a sample of M hidden neurons' activity configurations, $Y_t^k \sim P(Y_t|X, \mathcal{W})$, each referred to as a "particle".

In order to produce this sample, it is advantageous to reformulate the sampling problem $Y_t \sim P(Y_t|X, \mathcal{W})$ in a more convenient way as such applying to the drawing of a sample of the complete neuronal activity configurations $\mathcal{X}_t$, in such a way that the activity of the parts of the neuronal population observed at time t match with the available observations data X_t. In this sense, we view the activity of the entire neuronal population $\mathcal{X}_t$ as the "hidden" state, and the mapping of $\mathcal{X}_t$ onto the subsets of the observed neurons, $\mathsf{X} : \mathcal{X}_t \mapsto X_t$, as the observations of that state. In this form, the problem becomes that of sampling the sequence of the hidden states $\mathcal{X}_t$ from a Hidden Markov Model given the observations X_t.

This problem now can be efficiently solved using the standard forward-backward algorithm.

The forward-backward algorithm consists of two passes. In the first forward pass, a sequence of samples of the hidden states is produced according to $P(\mathcal{X}_t|X_{1:t}, \mathcal{W})$, where $X_{1:t}$ refers to the collection of all observed neuronal activities up to and including time t. Each sample in that sequence contains M examples of the complete neuronal population activity, $\mathcal{X}_t \sim P(\mathcal{X}_t|X_{1:t}, \mathcal{W})$ satisfying the constraint $\mathsf{X}(\mathcal{X}_t) = X_t$, while the entire sequence contains T such samples, $t = 1 \ldots T$, where T is the number of the observations, so that $\{\mathcal{X}_t^k, k = 1 \ldots M, t = 1 \ldots T\}$.

Forward pass samples can be constructed iteratively by drawing the initial sample $\mathcal{X}_0$ from a prior distribution $P(\mathcal{X}_0)$ and then constructing each next sample according to,

$$\mathcal{X}_t \sim P(\mathcal{X}_t|X_{1:t}) = \mathcal{Z}^{-1}\sum_{\mathcal{X}_{t-1}} P(X_t|\mathcal{X}_t)P(\mathcal{X}_t|\mathcal{X}_{t-1})P(\mathcal{X}_{t-1}|X_{1:t-1}). \tag{49}$$

Here $\mathcal{Z}$ is a normalization constant to be calculated below and we stopped writing parameter $\mathcal{W}$ in the probability densities for brevity.

According to Eq. (49), the forward step at each t can be realized by taking the previous sample's particles $\mathcal{X}_{t-1}^k \sim P(\mathcal{X}_{t-1}|X_{1:t-1})$ and "moving" them according to the transition probabilities

$$P(\mathcal{X}_{t-1}^k \to \mathcal{X}_t^k) = \mathcal{Z}^{-1} P(X_t|\mathcal{X}_t^k)P(\mathcal{X}_t^k|\mathcal{X}_{t-1}^k). \tag{50}$$

Eq. (50) can be simplified by noting that $P(X_t|\mathcal{X}_t)$ has the effect of only restricting the moves $\mathcal{X}_{t-1}^k \to \mathcal{X}_t^k$ to such that make the activity patterns of the neurons observed in $\mathcal{X}_t^k$ match the available observation X_t,

$$P(X_t|\mathcal{X}_t^k) \propto \begin{cases} 1\ if\ X_t^k = X_t \\ 0\ otherwise \end{cases} \tag{51}$$

By using this and taking advantage of the factorization of the probabilities $P(\mathcal{X}_t|\mathcal{X}_{t-1})$ over individual neurons i, $P(\mathcal{X}_t|\mathcal{X}_{t-1}) = \prod_i P(\mathcal{X}_{it}|\mathcal{X}_{t-1})$, we obtain the normalization constant $\mathcal{Z}$ explicitly as,

$$\mathcal{Z} = E_{\mathcal{X}_{t-1}}[P(X_t|\mathcal{X}_{t-1})] = \frac{1}{M}\sum_k P(X_t|\mathcal{X}_{t-1}^k). \tag{52}$$

With this simplification, we arrive at the final algorithm for the forward step:

Forward Step

(i) Select one $\mathcal{X}_{t-1}^k$ from the previous $t-1$ sample $\mathcal{X}_{t-1}^k \sim P(\mathcal{X}_{t-1}|X_{1:t-1})$ with probability

$$p(k) = 1/M \cdot P(X_t|\mathcal{X}_{t-1}^k)/\mathcal{Z} = P(X_t|\mathcal{X}_{t-1}^k)/\textstyle\sum_k P(X_t|\mathcal{X}_{t-1}^k);$$

where

$$P(X_t|\mathcal{X}_{t-1}) = \sum_{\mathcal{X}_t} P(X_t|\mathcal{X}_t)P(\mathcal{X}_t|\mathcal{X}_{t-1}).$$

(ii) Set in $\mathcal{X}_t^k$ the activity of the neurons i observed in observation t as $\mathcal{X}_{it}^k = X_{it}$;

(iii) Set in $\mathcal{X}_t^k$ the activity of the neurons i' not observed in observation t as $\mathcal{X}_{i't}^k \sim P(\mathcal{X}_{i't}|\mathcal{X}_{t-1}^k)$.

In the backward pass, the samples $(\mathcal{X}_{t-1}, \mathcal{X}_t) \sim P(\mathcal{X}_{t-1}, \mathcal{X}_t|X)$ need to be constructed for each t conditional

on all observations $X = \{X_t, t = 1 \dots T\}$. These samples can be constructed using the following relationship that we use from (Paninski et al. 2010),

$$P(\mathcal{X}_t, \mathcal{X}_{t+1}|X) = P(\mathcal{X}_t|X_{1:t}) \frac{P(\mathcal{X}_{t+1}|\mathcal{X}_t)}{P(\mathcal{X}_{t+1}|X_{1:t})} P(\mathcal{X}_{t+1}|X), \tag{53}$$

where $P(\mathcal{X}_{t+1}|X_{1:t}) = \sum_{\mathcal{X}_t} P(\mathcal{X}_{t+1}|\mathcal{X}_t) P(\mathcal{X}_t|X_{1:t}) = E_{\mathcal{X}_t}[P(\mathcal{X}_{t+1}|\mathcal{X}_t)]$, the average being over the forward pass sample $\mathcal{X}_t^k \sim P(\mathcal{X}_t|X_{1:t})$.

According to Eq. (53), the backward step can be constructed by first combining into pairs the forward pass samples for observation t, $\mathcal{X}_t^k \sim P(\mathcal{X}_t|X_{1:t})$, and the backward pass samples for observation $t+1$, $\mathcal{X}_{t+1}^l \sim P(\mathcal{X}_{t+1}|X)$, and then weighing these with the weights $w_t^{kl} = P(\mathcal{X}_{t+1}^l|\mathcal{X}_t^k)/\sum_k P(\mathcal{X}_{t+1}^l|\mathcal{X}_t^k)$. Thus formed pairs $(\mathcal{X}_t^k, \mathcal{X}_{t+1}^l)$ are distributed according to $(\mathcal{X}_t^k, \mathcal{X}_{t+1}^l) \sim P(\mathcal{X}_t|X_{1:t}) P(\mathcal{X}_{t+1}|X)$, and the expectation value of any functional $F(\mathcal{X}_t, \mathcal{X}_{t+1})$ over $P(\mathcal{X}_t, \mathcal{X}_{t+1}|X)$ can be calculated by using such pairs as $E[F] = 1/M \sum_{kl} F(\mathcal{X}_t^k, \mathcal{X}_{t+1}^l) w_t^{kl}$. In addition, $P(\mathcal{X}_t|X) = \sum_{\mathcal{X}_{t+1}} P(\mathcal{X}_t, \mathcal{X}_{t+1}|X)$ and the next backward pass sample for observation t, $\mathcal{X}_t^k \sim P(\mathcal{X}_t|X)$, can be constructed by drawing with replacement $\mathcal{X}_t^k$ from $(\mathcal{X}_t^k, \mathcal{X}_{t+1}^l)$ with probabilities $p(k) \propto \sum_l w_t^{kl}$.

Thus, we arrive at the final backward step algorithm as follows:

Backward Step

(i) Form M^2 pairs $(\mathcal{X}_t^k, \mathcal{X}_{t+1}^l)$ using the forward pass sample $\mathcal{X}_t^k \sim P(\mathcal{X}_t|X_{1:t})$ and the backward pass sample $\mathcal{X}_{t+1}^l \sim P(\mathcal{X}_{t+1}|X)$;

(ii) Calculate the weights $w_t^{kl} = P(\mathcal{X}_{t+1}^l|\mathcal{X}_t^k)/\sum_k P(\mathcal{X}_{t+1}^l|\mathcal{X}_t^k)$;

(iii) As the next backward pass sample $\mathcal{X}_t^l \sim P(\mathcal{X}_t|X)$ select with replacement $\mathcal{X}_t^k$ from the pairs $(\mathcal{X}_t^k, \mathcal{X}_{t+1}^l)$ with the probabilities $p(k) = 1/M \sum_l w_t^{kl}$;

(iv) The expectation value of a functional $F(\mathcal{X}_t, \mathcal{X}_{t+1})$, $E_{P(\mathcal{X}_t, \mathcal{X}_{t+1}|X)}[F(\mathcal{X}_t, \mathcal{X}_{t+1})]$, is given by $E[F] = 1/M \sum_{kl} F(\mathcal{X}_t^k, \mathcal{X}_{t+1}^l) w_t^{kl}$.

In the optimization step of the EM algorithm, we maximize with respect to $\mathcal{W}$ the following function,

$$\begin{aligned} Q(\mathcal{W}|\hat{\mathcal{W}}) &= E_{P(Y|X,\hat{\mathcal{W}})}[\log P(X, Y, \mathcal{W})] \\ &= \log P(\mathcal{W}) + E_{P(\mathcal{X}_0|X,\hat{\mathcal{W}})}[\log P(\mathcal{X}_0)] \\ &+ \sum_t E_{P(\mathcal{X}_{t-1}, \mathcal{X}_t|X,\hat{\mathcal{W}})}[\log P(\mathcal{X}_t|\mathcal{X}_{t-1}, \mathcal{W})]. \end{aligned} \tag{54}$$

In order to calculate $Q(\mathcal{W}|\hat{\mathcal{W}})$ it is sufficient to know the samples $(\mathcal{X}_t^k, \mathcal{X}_{t+1}^l) \sim P(\mathcal{X}_t|X_{1:t}) P(\mathcal{X}_{t+1}|X)$ and the weights w_t^{kl}. Moreover, $Q(\mathcal{W}|\hat{\mathcal{W}})$ can be split into a sum over the rows of the matrix $\mathcal{W}$, W_i, as $Q(\mathcal{W}|\hat{\mathcal{W}}) = \sum_i Q(W_i|\hat{\mathcal{W}})$, with $Q(W_i|\hat{\mathcal{W}})$ given by

$$\begin{aligned} Q(W_i|\hat{\mathcal{W}}) &= \log P(W_i) + E_{P(\mathcal{X}_0|X,\hat{\mathcal{W}})}[\log P(\mathcal{X}_{i0})] \\ &+ \sum_t E_{P(\mathcal{X}_{t-1}, \mathcal{X}_t|X,\hat{\mathcal{W}})}[\log P(\mathcal{X}_{it}|\mathcal{X}_{t-1}, W_i)]. \end{aligned} \tag{55}$$

Thus, the optimization of Eq. (54) can be solved for each row i independently, reducing the complexity of the optimization problem from quadratic in the number of neurons N to linear. Moreover, inhomogeneous Poisson point-process models of neuronal activity with log-concave rate functions such as the exponential $f(.) = \exp(.)$ result in $Q(W_i|\hat{\mathcal{W}})$ that are convex, which allows their numerical optimization to be solved efficiently for very large N, using the standard gradient descent methods (Boyd 2004).

Appendix B: Calculation of the partial observations log-likelihood in the linear neuronal activity model

In this appendix we calculate the integral

$$\begin{aligned} &P(Z_t, X_t|\hat{W}) \propto \\ &\int dY_t \exp\left(-(Z_t - W\mathcal{X}_t)^2/2 - \mathcal{X}_t^T C^{-1} \mathcal{X}_t/2\right), \end{aligned} \tag{56}$$

of the model (18), where the input neuronal activities are distributed according to a correlated Gaussian distribution with zero mean and the covariance matrix C,

$$P(\mathcal{X}_t) \propto \exp(-\mathcal{X}_t^T C^{-1} \mathcal{X}_t/2),$$

and the integration is performed over the part of $\mathcal{X}_t$, Y_t, that is not observed during observation t. The part of $\mathcal{X}_t$ observed during the observation t, respectively, is held fixed and equals X_t. W is a single row-vector from the full connectivity matrix $\mathcal{W}$ corresponding to the input connection weights of one "output" neuron.

The calculations in Eq. (56) can be simplified if we represent the integral in an invariant form by introducing δ-functions that will restrict the integration over $\mathcal{X}_t$ to the hyperplane defined by fixing X_t, namely,

$$\begin{aligned} &\int dY_t \exp\left(-(Z_t - W\mathcal{X}_t)^2/2 - \mathcal{X}_t^T C^{-1} \mathcal{X}_t/2\right) = \\ &\int d\mathcal{X}_t \prod_{i=1}^{i=m} \delta(\mathcal{X}_{it} - X_{it}) \\ &\times \exp\left(-(Z_t - W\mathcal{X}_t)^2/2 - \mathcal{X}_t^T C^{-1} \mathcal{X}_t/2\right). \end{aligned} \tag{57}$$

Here m is the number of the observed neuronal inputs and w.l.o.g. we assumed that the observed inputs X_t comprise the first m elements of $\mathcal{X}_t$. We now replace the δ-functions in Eq. (57) with their Fourier representation, $\delta(x) = \frac{1}{2\pi} \int dk e^{-ikx}$, yielding

$$\begin{aligned} &\int d\mathcal{X}_t dK \prod_{i=m+1}^{i=N} \delta(K_i) \exp\left(-(Z_t - W\mathcal{X}_t)^2/2\right. \\ &\left.-iK^T(\mathcal{X}_t - \bar{X}_t) - \mathcal{X}_t^T C^{-1} \mathcal{X}_t/2\right), \end{aligned} \tag{58}$$

where $\bar{X}_t$ is a full-size column-vector of neuronal inputs, with the first m elements equal to X_t and the rest of the elements zero (these do not affect the integral since $K_i = 0$ for $i > m$). In Eq. (58), the integral over $\mathcal{X}_t$ can be taken explicitly as a Gaussian, resulting in

$$\int dK \prod_{i=m+1}^{i=N} \delta(K_i) \exp(i\bar{X}_t^T K)\sqrt{\det \Gamma} \times \exp\left(-Z_t^2/2 + (Z_t W - iK^T)\Gamma(Z_t W^T - iK)/2\right), \tag{59}$$

where the matrix Γ is identified from the part of the argument of the exponential in Eq. (58) that is quadratic in $\mathcal{X}_t$, $\Gamma^{-1} = (C^{-1} + W^T W)$. We expand the second term under the exponential in Eq. (59) as

$$\int dK \prod_{i=m+1}^{i=N} \delta(K_i)\sqrt{\det \Gamma} \times \exp\left(-Z_t^2/2 + Z_t^2 W\Gamma W^T/2 + i\bar{X}_t^T K - iZ_t W\Gamma K - K^T\Gamma K/2\right). \tag{60}$$

The δ-functions in Eq. (60) subsequently restrict the integration over K to only such values where $K_i = 0$ for all $m < i \le N$. Thus, we rewrite this integration as

$$\int dK_X \sqrt{\det \Gamma} \times \exp\left(-Z_t^2/2 + Z_t^2 W\Gamma W^T/2 + i(\bar{X}_t^T - iZ_t W\Gamma)_X K_X - K_X^T \Gamma_X K_X/2\right), \tag{61}$$

where the subscript X means restriction to the first m elements, as contained in the observed set of neuronal inputs X_t. Thus obtained integration over K_X is again Gaussian, and so we can perform it explicitly producing

$$\int dY_t \exp(-(Z_t - W\mathcal{X}_t)^2/2 - \mathcal{X}_t^T C^{-1}\mathcal{X}_t/2) \propto \sqrt{\frac{\det\Gamma}{\det\Gamma_X}} \exp\left(-Z_t^2/2 + Z_t^2 W\Gamma W^T/2 - (\bar{X}_t^T - Z_t W\Gamma)_X \Gamma_X^{-1}(\bar{X}_t - Z_t\Gamma W^T)_X/2\right). \tag{62}$$

As a simple check, we take $C = I$ (uncorrelated inputs) and obtain by repeatedly using Woodbury lemma,

$$\begin{aligned} \Gamma &= (I + W^T W)^{-1} = I - W^T W/(1 + W^2) \\ \Gamma_X &= I - W_X^T W_X/(1 + W^2) \\ \Gamma_X^{-1} &= I + W_X^T W_X/(1 + W_Y^2) \\ (W\Gamma) &= W/(1 + W^2) \\ (W\Gamma)_X &= W_X/(1 + W^2) \end{aligned} \tag{63}$$

where W_X and W_Y are the restrictions of W to the subsets of the neuronal inputs X_t and Y_t, respectively, and $W^2 = WW^T$. For $\det\Gamma$ and $\det\Gamma_X$, we obtain $\det\Gamma = (1+W^2)^{-1}$ and $\det\Gamma_X = (1 + W_Y^2)/(1 + W^2)$, so that,

$$\det\Gamma/\det\Gamma_X = 1/(1 + W_Y^2).$$

Similarly,

$$\begin{aligned} &-Z_t^2 + Z_t^2 W\Gamma W^T = -Z_t^2/(1 + W^2) \\ &X_t^T\Gamma_X^{-1}X_t = X_t^2 + (W_X X_t)^2/(1 + W_Y^2) \\ &Z_t(W\Gamma)_X\Gamma_X^{-1}X_t = Z_t(W_X X_t)/(1 + W_Y^2) \\ &Z_t^2(W\Gamma)_X\Gamma_X^{-1}(\Gamma W^T)_X = -Z_t^2 W_X^2/((1 + W^2)(1 + W_Y^2)) \end{aligned} \tag{64}$$

Bringing everything in Eq. (64) together, we obtain for the case $C = I$,

$$\int dY_t \exp(-(Z_t - W\mathcal{X}_t)^2/2 - \mathcal{X}_t^T C^{-1}\mathcal{X}_t/2) = (1 + W_Y^2)^{-1/2} \exp\left(-\frac{1}{2}\left[\frac{Z_t^2}{1+W_Y^2} + \frac{2Z_t W_X X_t}{1+W_Y^2} - \frac{(W_X X_t)^2}{1+W_Y^2}\right] - \frac{X_t^2}{2}\right). \tag{65}$$

The correctness of the expression (65) can be verified by direct integration of the original integral using $C = I$, which is relatively simple.

For the case of general C, similarly by repeated use of Woodbury lemma we obtain

$$\begin{aligned} \Gamma &= C - C\frac{W^T W}{1+WCW^T}C \\ \Gamma_X &= C_{XX} - C_{X*}\frac{W^T W}{1+WCW^T}C_{*X} \\ \Gamma_X^{-1} &= C_{XX}^{-1} + C_{XX}^{-1}\frac{C_{X*}W^T W C_{*X}}{1+B^2}C_{XX}^{-1} \\ (W\Gamma) &= \frac{WC}{(1+WCW^T)} \\ (W\Gamma)_X &= \frac{WC_{*X}}{(1+WCW^T)} \end{aligned} \tag{66}$$

where

$$B^2 = WCW^T - WC_{*X}C_{XX}^{-1}C_{X*}W^T,$$

and C_{XX} is the square block of the full covariance matrix C corresponding to the observed inputs X_t, while C_{X*} and C_{*X} are the rectangular blocks of the full covariance matrix containing all the rows or the columns corresponding to the observed inputs X_t. Then, for the determinant factor we obtain,

$$\det\Gamma = \det C/(1 + WCW^T)$$

and

$$\det\Gamma_X = \det C_{XX}(1 + B^2)/(1 + WCW^T).$$

Consequently,

$$\sqrt{\frac{\det\Gamma}{\det\Gamma_X}} = \sqrt{\frac{\det C}{\det C_{XX}}} \cdot (1 + B^2)^{-1/2}. \tag{67}$$

By representing

$$C = \begin{bmatrix} C_{XX} & C_{XY} \\ C_{YX} & C_{YY} \end{bmatrix}$$

we can reorder the quantity B^2 as

$$B^2 = W_Y(C_{YY} - C_{YX}C_{XX}^{-1}C_{XY})W_Y^T.$$

We see then that B^2 plays the role here of W_Y^2 in Eq. (65). We further proceed to simplify the terms under the exponent

in Eq. (62) using Eq.(66). This highly tedious calculation results in the following,

$$\begin{aligned}&\int dY_t \exp(-(Z_t - W\mathcal{X}_t)^2/2 - \mathcal{X}_t^T C^{-1}\mathcal{X}_t/2) \propto \\ &\sqrt{\tfrac{\det C}{\det C_{XX}}}(1+B^2)^{-1/2} \\ &\times \exp\left(-\tfrac{1}{1+B^2}\tfrac{Z_t^2}{2} - \tfrac{1}{2}X_t^T C_{XX}^{-1} X_t \right. \\ &\left. + \tfrac{Z_t W C_{*X} C_{XX}^{-1} X_t}{1+B^2} - \tfrac{1}{2}\tfrac{(WC_{*X}C_{XX}^{-1}X_t)^2}{1+B^2} \right).\end{aligned} \tag{68}$$

As a consistency check, we verify that Eq. (68) reduces to Eq. (65) if $C = I$. Finally, we rewrite Eq. (68) more concisely as

$$\begin{aligned}&\int dY_t \exp(-(Z_t - W\mathcal{X}_t)^2/2 - \mathcal{X}_t^T C^{-1}\mathcal{X}_t/2) \propto \\ &\sqrt{\tfrac{\det C}{\det C_{XX}}}(1+B^2)^{-1/2} \\ &\times \exp\left(-\tfrac{1}{2}\tfrac{(Z_t - WC_{*X}C_{XX}^{-1}X_t)^2}{1+B^2} - \tfrac{1}{2}X_t^T C_{XX}^{-1} X_t \right)\end{aligned} \tag{69}$$

Appendix C: Additional proofs

In this appendix we present the complete proofs of some of the proposition found in the main text.

Theorem 1 (restated) *Let $P(\mathcal{X}|\mathcal{W})$ be a statistical model of neuronal population activity $\mathcal{X} = \{\mathcal{X}_t, t = 1, 2, \ldots\}$ and let $S = \{S_t, t = 1, 2, \ldots\}$, $S \sim P(S)$, be a series of partial observations of that model's activity over subpopulations of neurons S_t. Let $\mathcal{X}$ and S jointly define a stationary and ergodic stochastic process and assume that the classical MLE regularity conditions hold for the model $P(\mathcal{X}|\mathcal{W})$, namely:*

(A1) the parameter space $\mathcal{W} \in \mathfrak{W}$ is compact;
(A2) all distribution densities $P(\mathcal{X}_{t:t+k}|\mathcal{W})$ are continuous in $\mathcal{W}$;
(A3) $E\left[\left|\log P(X_{t:t+k|S_{t:t+k}}|\hat{\mathcal{W}})\right|\right] < \infty$ for all $\hat{\mathcal{W}}$ and $S_{t:t+k}$, where the expectation is over the stationary distribution $P(\mathcal{X}_{t:t+k}|\mathcal{W})$ for the true $\mathcal{W}$.

Assume further that the model $P(\mathcal{X}|\mathcal{W})$ is uniquely identified in the sense of Definition 1 by a set of distributions $\mathbf{P}(\mathbf{S}) = \{P(X_{t:t+k|S_{1:k+1}}|\mathcal{W}),\ S_{1:k+1} \in \mathbf{S}\}$ for some $\mathbf{S}$. Then, for any model of the partial observations $P(S)$ such that the support $\mathbf{S}' = \{S_{t:t+k} : P(S_{t:t+k}) > 0\}$ completely covers $\mathbf{S}$ in the sense of Definition 2, the ML estimator

$$\hat{\mathcal{W}}_T(\mathcal{X}, S) = \arg\max_{\hat{\mathcal{W}}} L(\hat{\mathcal{W}}|\mathcal{X}, S; T), \tag{70}$$

where

$$L(\hat{\mathcal{W}}|\mathcal{X}, S; T) = \sum_{t=1}^{t=T} \log P(X_{t:t+k|S_{t:t+k}}, S_{t:t+k}|\hat{\mathcal{W}}), \tag{71}$$

is consistent.

Proof Under the conditions of the theorem, consider the average log-likelihood function

$$l_T(\hat{\mathcal{W}}|\mathcal{X}, S) = \frac{1}{T}\sum_{t=1}^{t=T} \log P(X_{t:t+k|S_{t:t+k}}, S_{t:t+k}|\hat{\mathcal{W}}). \tag{72}$$

By the assumption of ergodicity, in the limit $T \to \infty$ almost surely

$$l_T(\hat{\mathcal{W}}|\mathcal{X}, S) \to E_{P(X_{t:t+k|S_{t:t+k}}, S_{t:t+k}|\mathcal{W})} \left\{\log P(X_{t:t+k|S_{t:t+k}}, S_{t:t+k}|\hat{\mathcal{W}})\right\}, \tag{73}$$

where $P(X_{t:t+k|S_{t:t+k}}, S_{t:t+k}|\mathcal{W})$ is the stationary distribution of the model under the true parameter $\mathcal{W}$. By construction, the tuples $S_{t:t+k}$ and $\mathcal{X}_{t:t+k}$ are statistically independent, therefore, we have in the limit $T \to \infty$,

$$l_\infty(\hat{\mathcal{W}}) = E_{P(S_{t:t+k})}\left\{E_{P(X_{t:t+k|S_{t:t+k}}|\mathcal{W})} \left[\log P(X_{t:t+k|S_{t:t+k}}|\hat{\mathcal{W}})\right]\right\} + const. \tag{74}$$

By the assumption of the coverage of the identifying set $\mathbf{P}(\mathbf{S})$ by the support of $P(S_{t:t+k})$ and Gibbs inequality, $l_\infty(\hat{\mathcal{W}})$ achieves maximum only and only when $\hat{\mathcal{W}} = \mathcal{W}$, providing for the identifiability condition of the MLE. Together with the regularity conditions (A1)-(A3), then, the series of estimates $\hat{\mathcal{W}}_T = \arg\max l_T(\hat{\mathcal{W}})$ converges in probability to $\hat{\mathcal{W}} = \arg\max l_\infty(\hat{\mathcal{W}}) = \mathcal{W}$ as $T \to \infty$. □

Lemma 1 (restated) *The expected log-likelihood function of model (18) is*

$$\begin{aligned}&l(\hat{W}_i, \hat{\Sigma}) = \\ &-1/2E\left\{\tfrac{1+W_i\Sigma W_i^T - 2\hat{W}_i\mathcal{A}_{X_k}W_i^T + \hat{W}_i\mathcal{A}'_{X_k}\hat{W}_i^T}{1+B_{ik}^2} \right. \\ &\left. + \log(1+B_{ik}^2)\right\} \\ &-1/2E\left\{Tr[\Sigma_{X_kX_K}\hat{\Sigma}_{X_kX_k}^{-1}] + \log\det\hat{\Sigma}_{X_kX_k}\right\},\end{aligned} \tag{75}$$

*where the subscript-notation in Σ refers to the blocks of Σ corresponding to the neuronal inputs identified by X_k and Y_k, with * referring to all row or column elements. B_{ik}^2, $\mathcal{A}_{X_k}$ and $\mathcal{A}'_{X_k}$ are*

$$\begin{aligned}\mathcal{A}_{X_k} &= \hat{\Sigma}_{*X_k}\hat{\Sigma}_{X_kX_k}^{-1}\Sigma_{X_k*} \\ \mathcal{A}'_{X_k} &= \hat{\Sigma}_{*X_k}\hat{\Sigma}_{X_kX_k}^{-1}\Sigma_{X_kX_k}\hat{\Sigma}_{X_kX_k}^{-1}\hat{\Sigma}_{X_k*} \\ B_{ik}^2 &= \hat{W}_i(\hat{\Sigma} - \hat{\Sigma}_{*X_k}\hat{\Sigma}_{X_kX_k}^{-1}\hat{\Sigma}_{X_k*})\hat{W}_i^T\end{aligned} \tag{76}$$

W_i and Σ are the true connection weights and the covariance matrix, respectively, and the average is over all different subsets of observed neurons X_k.

Proof Consider the average log-likelihood function given the T_i realizations $Z_i = \{Z_{ik}, k = 1 \ldots T_i\}$ and $X =$

$\{X_k, k = 1 \ldots T_i\}$ from model (18), marginal over the missing data $Y = \{Y_k, k = 1 \ldots T_i\}$,

$$l(W_i, \Sigma | Z_i, X) = \frac{1}{T_i} \log P(Z_i, X | W_i, \Sigma), \tag{77}$$

where $P(Z_i, X|W_i, \Sigma) = \int dY\, P(Z_i, X, Y|W_i, \Sigma)$. Note that Z_i and X in Eq. (77) are the collections of T_i realizations and so the RHS of Eq. (77) is dependent on T_i in this manner. Also note that Z_i and X are the observed data in this setting, and Y is the missing data to be integrated out.

When the number of realizations T_i is large, by the law of large numbers the RHS of Eq. (77) can be seen to converge in probability to the expected value of $\log P(Z_{ik}, X_k|W_i, \Sigma)$ under the true distribution of the inputs and outputs $P(Z_{ik}, X_k)$,

$$\begin{aligned} &l(\hat{W}_i, \hat{\Sigma} | Z_i, X) = \tfrac{1}{T_i} \log P(Z_i, X | \hat{W}_i, \hat{\Sigma}) \\ &= \tfrac{1}{T_i} \sum_{k=1}^{k=T_i} \log P(Z_{ik}, X_k | \hat{W}_i, \hat{\Sigma}) \\ &\to E_{P(Z_{ik}, X_k)}[\log P(Z_{ik}, X_k | \hat{W}_i, \hat{\Sigma})]. \end{aligned} \tag{78}$$

In the last line of Eq. (78) we recognize the expected log-likelihood function,

$$\begin{aligned} &l(\hat{W}_i, \hat{\Sigma}) = \\ &E[\log \textstyle\int dY_k\, P(Z_{ik}, X_k, Y_k | \hat{W}_i, \hat{\Sigma})], \end{aligned} \tag{79}$$

where the expectation, again, is with respect to the true density of the observed input and output variables, X_k and Z_{ik}, and we used

$$\begin{aligned} &P(Z_{ik}, X_k | \hat{W}_i, \hat{\Sigma}) = \\ &\textstyle\int dY_k\, P(Z_{ik}, X_k, Y_k | \hat{W}_i, \hat{\Sigma}). \end{aligned} \tag{80}$$

We see now that it is necessary to calculate

$$\begin{aligned} &P(Z_{ik}, X_k | \hat{W}_i, \hat{\Sigma}) = \\ &\textstyle\int dY_k \exp\Big(-(Z_{ik} - \hat{W}_{iX_k} X_k - \hat{W}_{iY_k} Y_k)^2/2 \\ &-\mathcal{X}_k^T \hat{\Sigma}^{-1} \mathcal{X}_k/2 + const\Big), \end{aligned} \tag{81}$$

where $\mathcal{X}_k$ is the vector of the complete input activities formed by suitably combining X_k and Y_k, that is, $\mathcal{X}_k = [X_k; Y_k]$. The integral in Eq. (81) can be calculated explicitly, although the respective calculation is lengthy and is presented fully in Appendix B. The result of that calculation is

$$\begin{aligned} &\log P(Z_{ik}, X_k | \hat{W}_i, \hat{\Sigma}) = \\ &-1/2(1 + B_{ik}^2)^{-1} (Z_{ik} - \hat{W}_i \hat{\Sigma}_{*X_k} \hat{\Sigma}_{X_k X_k}^{-1} X_k)^2 \\ &-1/2 \log(1 + B_{ik}^2) - X_k^T \hat{\Sigma}_{X_k X_k}^{-1} X_k/2 \\ &-1/2 \log\det \hat{\Sigma}_{X_k X_k} + const, \end{aligned} \tag{82}$$

where the scalars B_{ik}^2 are defined by

$$\begin{aligned} B_{ik}^2 &= \hat{W}_i \hat{\Sigma} \hat{W}_i^T - \hat{W}_i \hat{\Sigma}_{*X_k} \hat{\Sigma}_{X_k X_k}^{-1} \hat{\Sigma}_{X_k *} \hat{W}_i^T \\ &= \hat{W}_{iY_k} (\hat{\Sigma}_{Y_k Y_k} - \hat{\Sigma}_{Y_k X_k} \hat{\Sigma}_{X_k X_k}^{-1} \hat{\Sigma}_{X_k Y_k}) \hat{W}_{iY_k}^T, \end{aligned}$$

and the subscripted notation in Σ refers to the blocks of Σ corresponding to the neuronal inputs identified by X_k and Y_k. For example, $\Sigma_{X_k X_k}$ is the submatrix of Σ composed of all elements of Σ located at the intersection of the rows and columns identified by X_k. Similarly, Σ_{*X_k} is the rectangular submatrix of Σ containing all the columns corresponding to the observed inputs X_k, and $\Sigma_{X_k *}$ is a similar rectangular submatrix of all the X_k-rows of Σ.

Using Eq. (82), we can now obtain the final expression for the expected log-likelihood $l(\hat{W}_i, \hat{\Sigma})$,

$$\begin{aligned} &l(\hat{W}_i, \hat{\Sigma}) = \\ &-1/2E\left[\frac{(Z_{ik} - \hat{W}_i \hat{\Sigma}_{*X_k} \hat{\Sigma}_{X_k X_k}^{-1} X_k)^2}{1 + B_{ik}^2} + \log(1 + B_{ik}^2)\right. \\ &\left. + X_k^T \hat{\Sigma}_{X_k X_k}^{-1} X_k + \log\det \hat{\Sigma}_{X_k X_k}\right], \end{aligned} \tag{83}$$

where the expectation is again under the true distribution of the observed inputs and outputs. We now take the average in Eq. (83) over all X_k where the set of neurons contained in X_k is the same. This leads to the following expression,

$$\begin{aligned} &l(\hat{W}_i, \hat{\Sigma}) = \\ &-1/2E\left\{\frac{1 + W_i \Sigma W_i^T - 2\hat{W}_i \mathcal{A}_{X_k} W_i^T + \hat{W}_i \mathcal{A}'_{X_k} \hat{W}_i^T}{1 + B_{ik}^2}\right. \\ &\left. + \log(1 + B_{ik}^2)\right\} \\ &-1/2E\left\{Tr[\Sigma_{X_k X_k} \hat{\Sigma}_{X_k X_k}^{-1}] + \log\det \hat{\Sigma}_{X_k X_k}\right\}, \end{aligned} \tag{84}$$

where $\mathcal{A}$ and $\mathcal{A}'$ are

$$\begin{aligned} \mathcal{A}_{X_k} &= \hat{\Sigma}_{*X_k} \hat{\Sigma}_{X_k X_k}^{-1} \Sigma_{X_k *} \\ \mathcal{A}'_{X_k} &= \hat{\Sigma}_{*X_k} \hat{\Sigma}_{X_k X_k}^{-1} \Sigma_{X_k X_k} \hat{\Sigma}_{X_k X_k}^{-1} \hat{\Sigma}_{X_k *}, \end{aligned} \tag{85}$$

and W_i and Σ are the true connection weights and the true covariance matrix parameters, respectively. The remaining average in Eq. (84) is over all different subsets of the observed inputs X_k. □

Theorem 3 (restated) *Consider a family of general "network type" Markov models of neuronal population activity characterized by a $N \times N$ connectivity matrix $\mathcal{W}$ and a transition probability density*

$$P(\mathcal{X}_t | \mathcal{X}_{t-1}; \mathcal{W}) = \prod_{i=1}^{i=N} P(\mathcal{X}_{it} | W_i \mathcal{X}_{t-1}), \tag{86}$$

where W_i is the i^{th} row of $\mathcal{W}$ and $N = dim(\mathcal{X}_t)$. Let model (86) define an ergodic stochastic process and let $\log P(\mathcal{X}_t|\mathcal{X}_{t-1}; \mathcal{W})$ be L_1 integrable under the stationary distribution of that process. Also, let $l_{T,N}(\mathcal{W}|\mathcal{X})$ be the average log-likelihood function for the realizations of the neuronal activity patterns $\mathcal{X} = \{\mathcal{X}_t, t = 1 \ldots T\}$ in model (86),

$$l_{T,N}(\mathcal{W}|\mathcal{X}) = \tfrac{1}{NT} \sum_{t=1}^{t=T} \sum_{i=1}^{i=N} \log P(\mathcal{X}_{it} | \mathcal{X}_{t-1}; \mathcal{W}). \tag{87}$$

In that case, if the sums

$$\mathcal{J}_{it} = \sum_{j=1}^{j=N} w_{ij}\mathcal{X}_{j,t-1} \to \mathcal{N}(m_i, \sigma_i^2) \tag{88}$$

in distribution as $N \to \infty$ *for tuples* $\mathcal{X}_{t-1}$ *from* $P(\mathcal{X}_{t-1})$ *and some* m_i *and* σ_i*, possibly functions of* N *(the Central Limit Theorem), then the set of all triple-distributions* $P(\mathcal{X}_{i,t+1}, \mathcal{X}_{jt}, \mathcal{X}_{kt})$ *is uniquely identifying for model (86) in the limit* $N \to \infty$ *and, furthermore,* $l_{T,N}(\mathcal{W}|\mathcal{X}) \to l_\infty(\mathcal{W})$ *almost surely as* $T, N \to \infty$*, where*

$$l_\infty(\mathcal{W}) = \frac{1}{N}\sum_{i=1}^{i=N} \int d\mathcal{X}_i d\mathcal{J}_i \frac{1}{(2\pi W_i \Sigma(\mathcal{X}_i) W_i^T)^{1/2}} \times \log P(\mathcal{X}_i|\mathcal{J}_i + W_i\mu(\mathcal{X}_i)) e^{-\mathcal{J}_i^2/(2W_i\Sigma(\mathcal{X}_i)W_i^T)} \tag{89}$$

and $\mu(\mathcal{X}_i) = E[\mathcal{X}_t|\mathcal{X}_{i,t+1} = \mathcal{X}_i]$ *and* $\Sigma(\mathcal{X}_i) = cov(\mathcal{X}_t|\,\mathcal{X}_{i,t+1} = \mathcal{X}_i)$.

Proof Consider the average log-likelihood function $l_{T,N}(\mathcal{W}|\mathcal{X})$ given by Eq. (87). By the Ergodic theorem, each i-term in Eq. (87) converges almost surely as $T \to \infty$ to

$$\frac{1}{T}\sum_{t=1}^{t=T} \log P(\mathcal{X}_{it}|\mathcal{J}_{it}) \to \int d\mathcal{X}_i d\mathcal{J}_i \log P(\mathcal{X}_{it}|\mathcal{J}_{it}) P(\mathcal{X}_i, \mathcal{J}_i), \tag{90}$$

where $P(\mathcal{X}_i, \mathcal{J}_i)$ is the joint distribution of $\mathcal{J}_{it}$ and $\mathcal{X}_{it}$ given the stationary distribution $P(\mathcal{X}_t)$. We rewrite $P(\mathcal{X}_i, \mathcal{J}_i) = P(\mathcal{J}_i|\mathcal{X}_i)P(\mathcal{X}_i)$ and take advantage of the assumption of the validity of the Central Limit Theorem for the sums $\mathcal{J}_{it}$, by which $P(\mathcal{J}_i|\mathcal{X}_i)$ approaches the Normal distribution as $N \to \infty$ with the mean $m_i = W_i\mu(\mathcal{X}_i)$ and the variance $\sigma_i^2 = W_i\Sigma(\mathcal{X}_i)W_i^T$. Then, if first T and then N tends to infinity, $l_{T,N}(\mathcal{W}|\mathcal{X})$ tends to

$$l_{T,N}(\mathcal{W}|\mathcal{X}) \to \frac{1}{N}\sum_{i=1}^{i=N} \int d\mathcal{X}_i d\mathcal{J}_i \frac{1}{(2\pi W_i \Sigma(\mathcal{X}_i) W_i^T)^{1/2}} \times \log P(\mathcal{X}_i|\mathcal{J}_i) e^{-(\mathcal{J}_i - m_i)^2/(2W_i\Sigma(\mathcal{X}_i)W_i^T)}. \tag{91}$$

From Eq. (91) it is seen that $\mu(\mathcal{X}_i)$ and $\Sigma(\mathcal{X}_i)$ are the sufficient statistics of model (86) in the limit $N \to \infty$. Furthermore, $\mu(\mathcal{X}_i)$ and $\Sigma(\mathcal{X}_i)$ are defined by the set of all distributions $P(\mathcal{X}_{i,t+1}, \mathcal{X}_{jt}, \mathcal{X}_{kt})$. Then, the set of all distributions $P(\mathcal{X}_{i,t+1}, \mathcal{X}_{jt}, \mathcal{X}_{kt})$ is uniquely identifying for model (86) in the limit $N \to \infty$, by Corollary 1. □

References

Abeles, M. (1991). *Corticonics*: Cambridge University Press.

Bellet, L.R. (2006). Ergodic properties of Markov processes. In *Open Quantum Systems II* (pp. 1–39). Berlin: Springer.

Berk, K.N. (1973). A Central Limit Theorem for m-Dependent Random Variables with Unbounded m. *Annals of Probability*, *1*(2), 352–354.

Boyd, S.P. (2004). *Convex optimization*: Cambridge University Press.

Bradley, R.C. (2005). Basic properties of strong mixing conditions. A survey and some open questions. *Probability surveys*, *2*, 107–144.

Braitenberg, V., & Schuz, A. (1998). *Cortex: statistics and geometry of neuronal connectivity*. Berlin: Springer.

Brillinger, D. (1988). Maximum likelihood analysis of spike trains of interacting nerve cells. *Biological Cyberkinetics*, *59*, 189–200.

Brillinger, D. (1992). Nerve cell spike train data analysis: a progression of technique. *Journal of the American Statistical Association*, *87*, 260–271.

Chornoboy, E., Schramm, L., & Karr, A. (1988). Maximum likelihood identification of neural point process systems. *Biological Cybernetics*, *59*, 265–275.

Cotton, R.J., Froudarakis, E., Storer, P., Saggau, P., & Tolias, A.S. (2013). Three-dimensional mapping of microcircuit correlation structure. *Frontiers in Neural Circuits*, *7*, 151.

Cossart, R., Aronov, D., & Yuste, R. (2003). Attractor dynamics of network up states in the neocortex. *Nature*, *423*, 283–288.

Coulon-Prieur, C., & Doukhan, P. (2000). A triangular central limit theorem under a new weak dependence condition. *Stat. Probab. Lett.*, *27*(1), 61–68.

Davidson, J. (2006). Asymptotic methods and functional central limit theorems. In T.C. Mills, & K. Patterson (Eds.), *Palgrave Handbooks of Econometrics*: Palgrave-Macmillan.

Dedecker, J., & Merlevede, F. (2002). Necessary and sufficient conditions for the conditional central limit theorem. *Annals of Probability*, *30*, 1044–1081.

Dempster, A., Laird, N., & Rubin, D. (1977). Maximum likelihood from incomplete data via the EM algorithm. *Journal of the Royal Statistical Society, Series B*, *39*, 1–38.

Djurisic, M., Antic, S., Chen, W.R., & Zecevic, D. (2004). Voltage imaging from dendrites of mitral cells: EPSP attenuation and spike trigger zones. *Journal of Neuroscience*, *24*(30), 6703–6714.

Furedi, Z., & Komlos, J. (1981). The eigenvalues of random symmetric matrices. *Combinatorica*, *1*, 233.

Doukhan, P. (1994). *Mixing: Properties and Examples*: Springer. Lect. Notes. Stat. 85.

Godsill, S., Doucet, A., & West, M. (2001). Maximum a Posteriori Sequence Estimation Using Monte Carlo Particle Filters. *Annals of the Institute of Statistical Mathematics*, *53*(1), 82–96.

Gomez-Urquijo, S.M., Reblet, C., Bueno-Lopez, J.L., & Gutierrez-Ibarluzea, I. (2000). Gabaergic neurons in the rabbit visual cortex: percentage, distribution and cortical projections. *Brain Research*, *862*, 171–9.

Grewe, B., Langer, D., Kasper, H., Kampa, B., & Helmchen, F. (2010). High-speed *in vivo* calcium imaging reveals neuronal network activity with near-millisecond precision. *Nature Methods*, 399–405.

Guillotin-Plantard, N., & Prieur, C. (2010). Central limit theorem for sampled sums of dependent random variables. *ESAIM: Probability and Statistics*, *14*, 299–314.

Hairer, M. (2010). "Convergence of Markov processes." Lecture notes.

Hall, P., & Heyde, C.C. (2014). *Martingale limit theory and its applications*, (p. 320): Academic Press. Chapter 3.

Iyer, V., Hoogland, T.M., & Saggau, P. (2006). Fast functional imaging of single neurons using random-access multiphoton (RAMP) microscopy. *Journal of Neurophysiology*, *95*(1), 535–545.

Johnson, O. (2001). An Information-Theoretic Central Limit Theorem for Finitely Susceptible FKG Systems. *Theory Probab. Appl.*, *50*(2), 214–224.

Kantas, N., Doucet, A., Singh, S.S., & Maciejowski, J.H. (2009). An overview of sequential Monte Carlo methods for parameter estimation in general state-space models. In *15th IFAC Symposium on System Identification (SYSID), Saint-Malo, France, 2009 Jul 6*, (Vol. 102 p. 117).

Keshri, S., Pnevmatikakis, E., Pakman, A., Shababo, B., & Paninski, L. (2013). A shotgun sampling solution for the common input problem in neuronal connectivity inference. arXiv:1309.3724.

Klartag, B. (2007). A central limit theorem for convex sets. *Inventiones Mathematicae*, *168*, 91–131.

Koch, C. (1999). *Biophysics of Computation*: Oxford University Press.

Kulkarni, J., & Paninski, L. (2007). Common-input models for multiple neural spike-train data. *Network: Computation in Neural Systems*, *18*, 375–407.

Lefort, S., Tomm, C., Floyd Sarria, J.-C., & Petersen, C.C.H. (2009). The excitatory neuronal network of the c2 barrel column in mouse primary somatosensory cortex. *Neuron*, *61*, 301–16.

Lehmann, E.L. (1999). *Elements of large-sample theory*. New York: Springer. Chapter 2.8.

Mishchenko, Y., Vogelstein, J., & Paninski, L. (2011). A Bayesian approach for inferring neuronal connectivity from calcium fluorescent imaging data. *Annals of Applied Statistics*, *5*, 1229–61.

Mishchenko, Y., & Paninski, L. (2011). Efficient methods for sampling spike trains in networks of coupled neurons. *The Annals of Mathematical Statistics*, *5*(3), 1893–1919.

Newman, C. (1984). Asymptotic Independence and Limit Theorems for Positively and Negatively Dependent Random Variables. *Lecture Notes-Monograph Series*, 127–140.

Neumann, M.H. (2013). A central limit theorem for triangular arrays of weakly dependent random variables, with applications in statistics. *ESAIM: Probability and Statistics*, *17*, 120–134.

Nguyen, Q.T., Callamaras, N., Hsieh, C., & Parker, I. (2001). Construction of a two-photon microscope for video-rate Ca^2+ imaging. *Cell Calcium*, *30*(6), 383–393.

Nykamp, D. (2007). A mathematical framework for inferring connectivity in probabilistic neuronal networks. *Mathematical Biosciences*, *205*, 204–251.

Nykamp, D.Q. (2005). Revealing pairwise coupling in linear-nonlinear networks. *SIAM Journal of Applied Mathematics*, *65*(6), 2005–2032.

Ohki, K., Chung, S., Ch'ng, Y., Kara, P., & Reid, C. (2005). Functional imaging with cellular resolution reveals precise micro-architecture in visual cortex. *Nature*, *433*, 597–603.

Paninski, L. (2004). Maximum likelihood estimation of cascade point-process neural encoding models. *Network: Computation in Neural Systems*, *15*, 243–262.

Paninski, L., Ahmadian, Y., Ferreira, D., Koyama, S., Rahnama, K., Vidne, M., Vogelstein, J., & Wu, W. (2010). A new look at state-space models for neural data. *Journal of Computational Neuroscience*, *29*, 107–126.

Paninski, L., Fellows, M., Shoham, S., Hatsopoulos, N., & Donoghue, J. (2004). Superlinear population encoding of dynamic hand trajectory in primary motor cortex. *Journal of Neuroscience*, *24*, 8551–8561.

Pillow, J., & Latham, P. (2007). Neural characterization in partially observed populations of spiking neurons. NIPS.

Pillow, J., Shlens, J., Paninski, L., Sher, A., Litke, A., Chichilnisky, E., & Simoncelli, E. (2008). Spatiotemporal correlations and visual signaling in a complete neuronal population. *Nature*, *454*, 995–999.

Plesser, H., & Gerstner, W. (2000). Noise in integrate-and-fire neurons: From stochastic input to escape rates. *Neural Computation*, *12*, 367–384.

Rabiner, L.R. (1989). A Tutorial on Hidden Markov Models and Selected Applications in Speech Recognition. *Proceedings of the IEEE*, *72*(2), 257–286.

Rasmussen, C.E., & Williams, C.K.I. (2006). Gaussian processes for Machinee Learning. MIT Press: Appendix B.

Reddy, G., Kelleher, K., Fink, R., & Saggau, P. (2008a). Three-dimensional random access multiphoton microscopy for functional imaging of neuronal activity. *Nature neuroscience*, *11*, 713–720.

Reddy, G., Kelleher, K., Fink, R., & Saggau, P. (2008b). Three-dimensional random access multiphoton microscopy for functional imaging of neuronal activity. *Nature Neuroscience*, *11*(6), 713–720.

Rigat, F., de Gunst, M., & van Pelt, J. (2006). Bayesian modelling and analysis of spatio-temporal neuronal networks. *Bayesian Analysis*, *1*, 733–764.

Salome, R., Kremer, Y., Dieudonne, S., Leger, J.-F., Krichevsky, O., Wyart, C., Chatenay, D., & Bourdieu, L. (2006). Ultrafast random-access scanning in two-photon microscopy using acousto-optic deflectors. *Journal of Neuroscience Methods*, *154*(1–2), 161–174.

Sayer, R.J., Friedlander, M.J., & Redman, S.J. (1990). The time course and amplitude of epsps evoked at synapses between pairs of ca3/ca1 neurons in the hippocampal slice. *Journal of Neuroscience*, *10*, 826–36.

Soudry, D., Keshri, S., Stinson, P., Oh, M.-H., Iyengar, G., & Paninski, L. (2015). Efficient "Shotgun" inference of neural connectivity from highly sub-sampled activity data. *PLOS Computational Biology*, *11*, e1004464.

Stevenson, I., Rebesco, J., Hatsopoulos, N., Haga, Z., Miller, L., & Koerding, K. (2008a). Inferring network structure from spikes. Statistical Analysis of Neural Data meeting.

Stevenson, I.H., Rebesco, J.M., Hatsopoulos, N.G., Haga, Z., Miller, L.E., & Kording, K.P. (2009). Bayesian inference of functional connectivity and network structure from spikes. *IEEE Transactions on Neural Systems and Rehabilitation*, *17*, 203–13.

Stevenson, I.H., Rebesco, J.M., Miller, L.E., & Kording, K.P. (2008b). Inferring functional connections between neurons. *Current Opinion in Neurobiology*, *18*, 582–8.

Stosiek, C., Garaschuk, O., Holthoff, K., & Konnerth, A. (2003). *In vivo* two-photon calcium imaging of neuronal networks. *Proceedings of The National Academy Of Sciences Of The United States Of America*, *100*(12), 7319–7324.

Theis, L., Berens, P., Froudarakis, E., Reimer, J., Roman-Roson, M., Baden, T., Euler T., Tolias A.S., & Bethge, M. (2015). Supervised learning sets benchmark for robust spike detection from calcium imaging signals. *bioRxiv*, 010777.

Truccolo, W., Eden, U., Fellows, M., Donoghue, J., & Brown, E. (2005). A point process framework for relating neural spiking activity to spiking history, neural ensemble and extrinsic covariate effects. *Journal of Neurophysiology*, *93*, 1074–1089.

Tsien, R.Y. (1989). Fluorescent probes of cell signaling. *Annual Review of Neuroscience*, *12*, 227–253.

Turaga, S., Buesing, L., Packer, A., Dalgleish, H., Pettit, N., Hausser, M., & Macke, J. (2013). Inferring neural population dynamics from multiple partial recordings of the same neural circuit. NIPS.

Varadhan, S.R.S. (2001). *Probability theory, volume 7 of Courant Lecture Notes in Mathematics*. New York: New York University Courant Institute of Mathematical Sciences. Chapter 6.

Vidne, M., Ahmadian, Y., Shlens, J., Pillow, J., Kulkarni, J., Litke, A., Chilchilnisky, E., Simoncelli, E., & Paninski, L. (2012). The impact of common noise on the activity of a large network of retinal ganglion cells. *Journal of Computational Neuroscience*, *33*, 97–121.

Vidne, M., Kulkarni, J., Ahmadian, Y., Pillow, J., Shlens, J., Chichilnisky, E., Simoncelli, E., & Paninski, L. (2009). Inferring functional connectivity in an ensemble of retinal ganglion cells sharing a common input. COSYNE.

Vogelstein, J., Watson, B., Packer, A., Yuste, R., Jedynak, B., & Paninski, L. (2009). Spike inference from calcium imaging using sequential Monte Carlo methods. *Biophysical Journal*, *97*, 636.

Vogelstein, J.T., Packer, A.M., Machado, T.A., Sippy, T., Babadi, B., Yuste, R., & Paninski, L. (2010). Fast nonnegative deconvolution

for spike train inference from population calcium imaging. *Journal of Neurophysiology*, *104*, 3691.

Wallace, D., zum Alten Borgloh, S., Astori, S., Yang, Y., Bausen, M., K"ugler, S., Palmer, A., Tsien, R., Sprengel, R., Kerr, J., Denk, W., & Hasan, M. (2008). Single-spike detection *in vitro* and *in vivo* with a genetic Ca2+ sensor. *Nature Methods*, *5*(9), 797–804.

Yatsenko, D., Josi, K., Ecker, A.S., Froudarakis, E., Cotton, R.J., & Tolias, A.S. (2015). Improved Estimation and Interpretation of Correlations in Neural Circuits. *PLoS Computational Biology*, *11*, e1004083.

Yuste, R., Konnerth, A., Masters, B., & et al. (2006). Imaging in Neuroscience and Development, A Laboratory Manual.